The CDF Run II Silicon Vertex Detectors: operational experience, aging studies and trigger applications

Benedetto Di Ruzza

Brookhaven National Laboratory March 2th 2012

Introduction

I'm working in CDF since 2004.

I had my Ph.D. working in the measurement of the branching ratio of the Bs to phi, phi decay in CDFII:
http://www-cdf.fnal.gov/physics/new/bottom/090618.blessed-Bsphiphi2.9/

event selection

the measurement method

$$\frac{BR(B_s \mapsto \phi\phi)}{BR(B_s \mapsto J/\psi\,\phi)} = \frac{N_{\phi\phi}}{N_{J/\psi\phi}} \cdot \frac{\epsilon_{(B_s \mapsto J/\psi\phi)}}{\epsilon_{(B_s \mapsto \phi\phi)}} \cdot \frac{BR(J/\psi \mapsto \mu\mu)}{BR(\phi \mapsto KK)} \cdot \epsilon_\mu$$

the decay

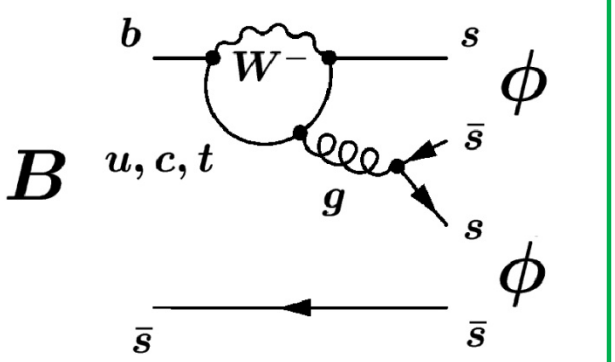

the result

$$\frac{\mathcal{B}(B_s^0 \to \phi\phi)}{\mathcal{B}(B_s^0 \to J/\psi\phi)} = [1.78 \pm 0.14(stat) \pm 0.20(syst)] \cdot 10^{-2}$$

$$\mathcal{B}(B_s^0 \to \phi\phi) = [2.40 \pm 0.21(stat) \pm 0.27(syst) \pm 0.82(BR)] \cdot 10^{-5}$$

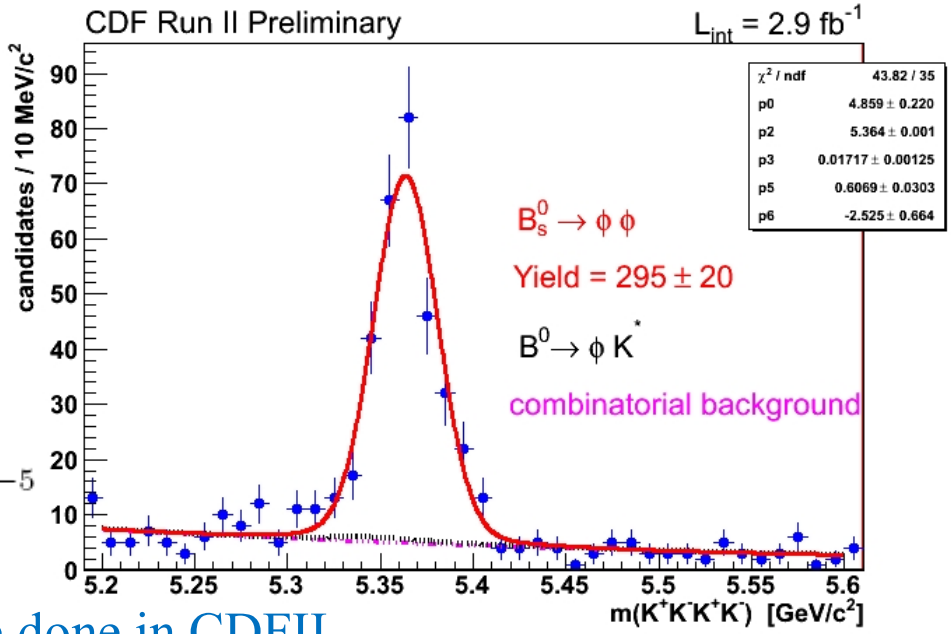

…..but this talk I will describe the other things I have done in CDFII

OUTLINE

1) The CDF II detector
2) The CDF II silicon sub-detectors
3) Silicon sensors aging studies
4) The Secondary Vertex online Trigger (SVT) at CDFII
5) Impact on the physics results

The Tevatron and the CDFII detector

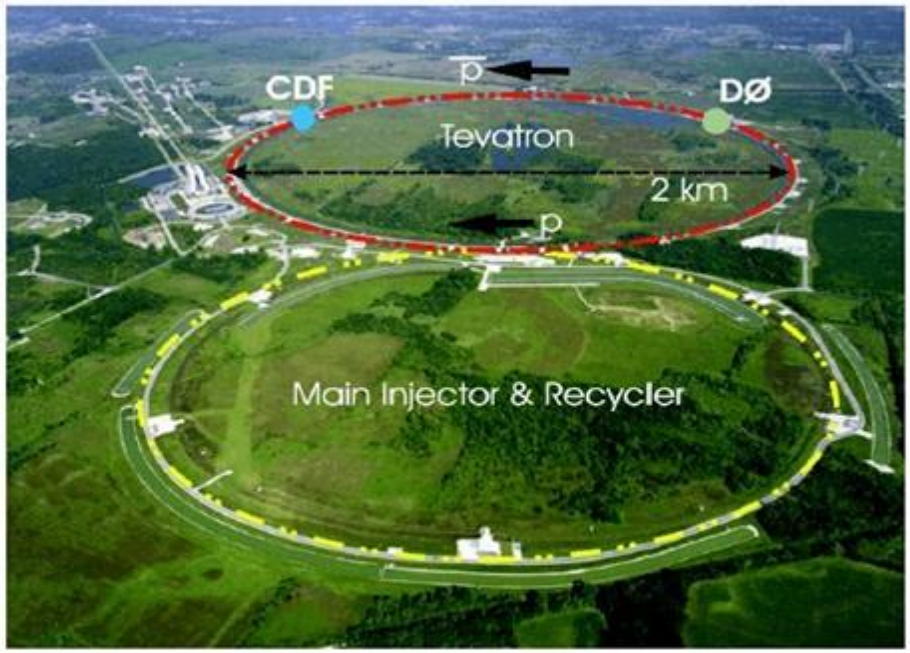

- **Tevatron:** proton-antiproton collider at $\sqrt{s} = 1.96$ TeV

Two multi-purpose detectors: CDF & DØ

- **CDF II:** Multilayered HEP detector with excellent tracking
  - ✓ silicon detectors designed for ~3 fb^{-1}
  - ✓ large open-cell drift chamber

The Tevatron and the CDFII detector

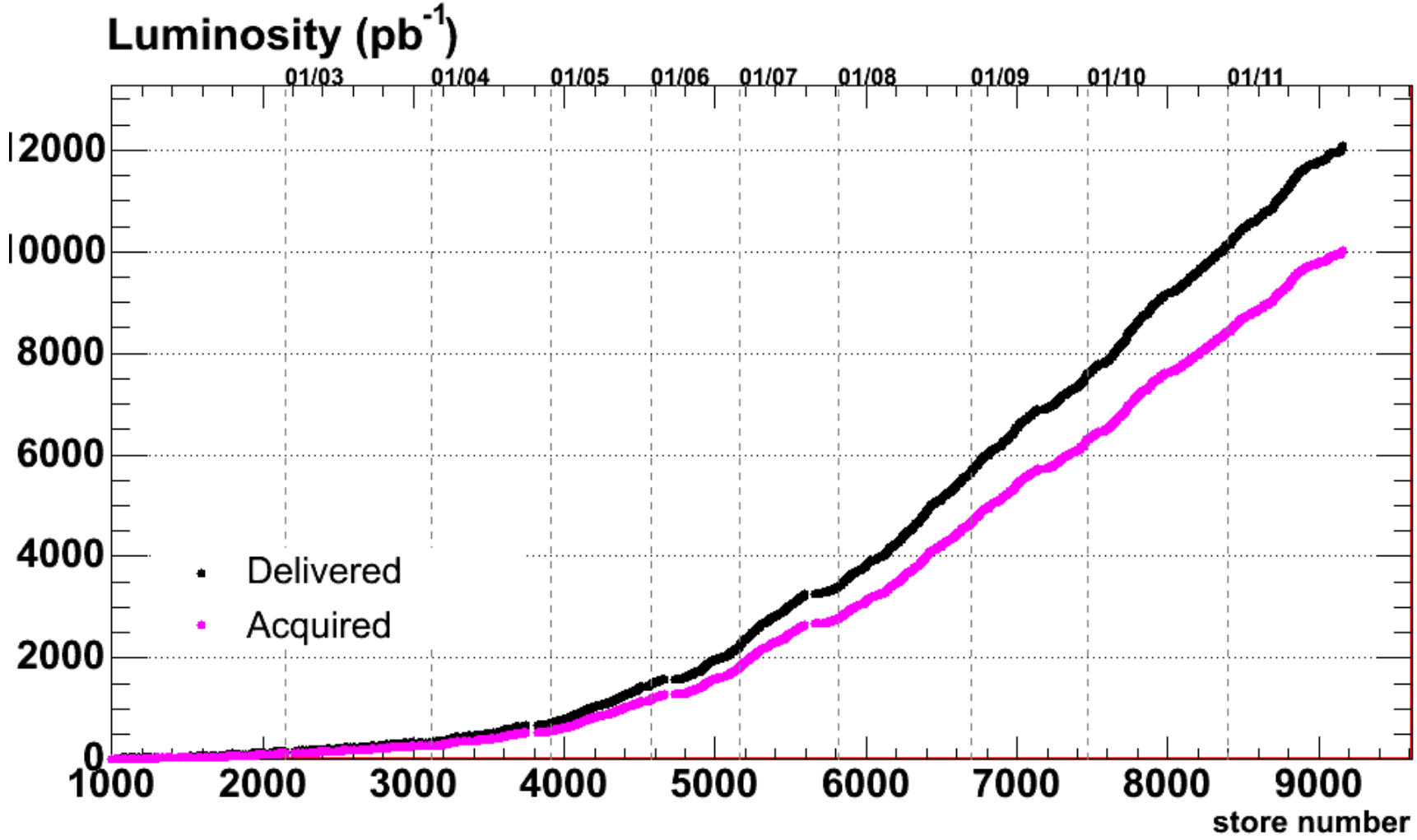

– Delivered: 11.995 fb-1
– Live: 9.977 fb-1(83.2%)

The CDFII Detector

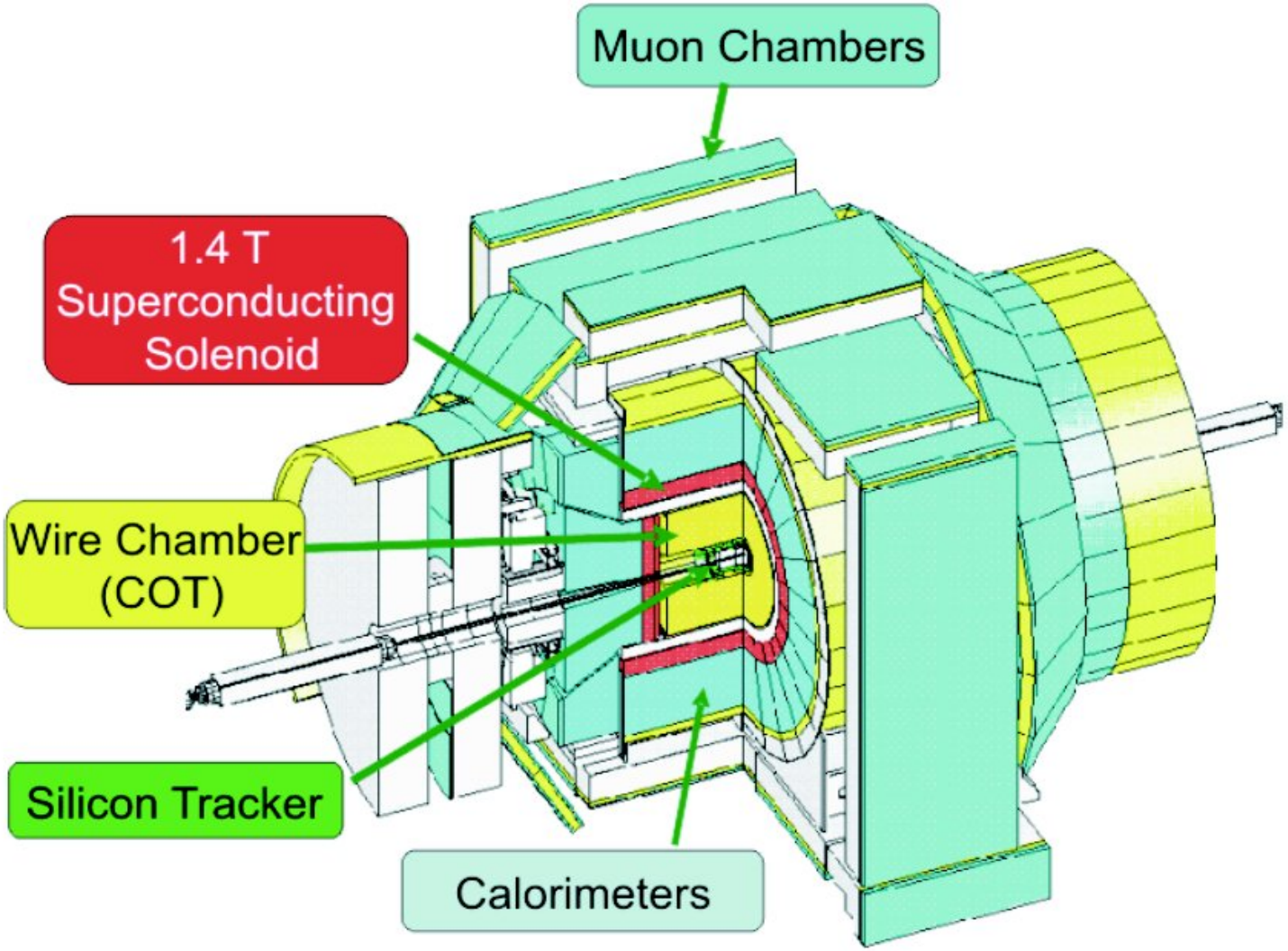

The Silicon Detectors

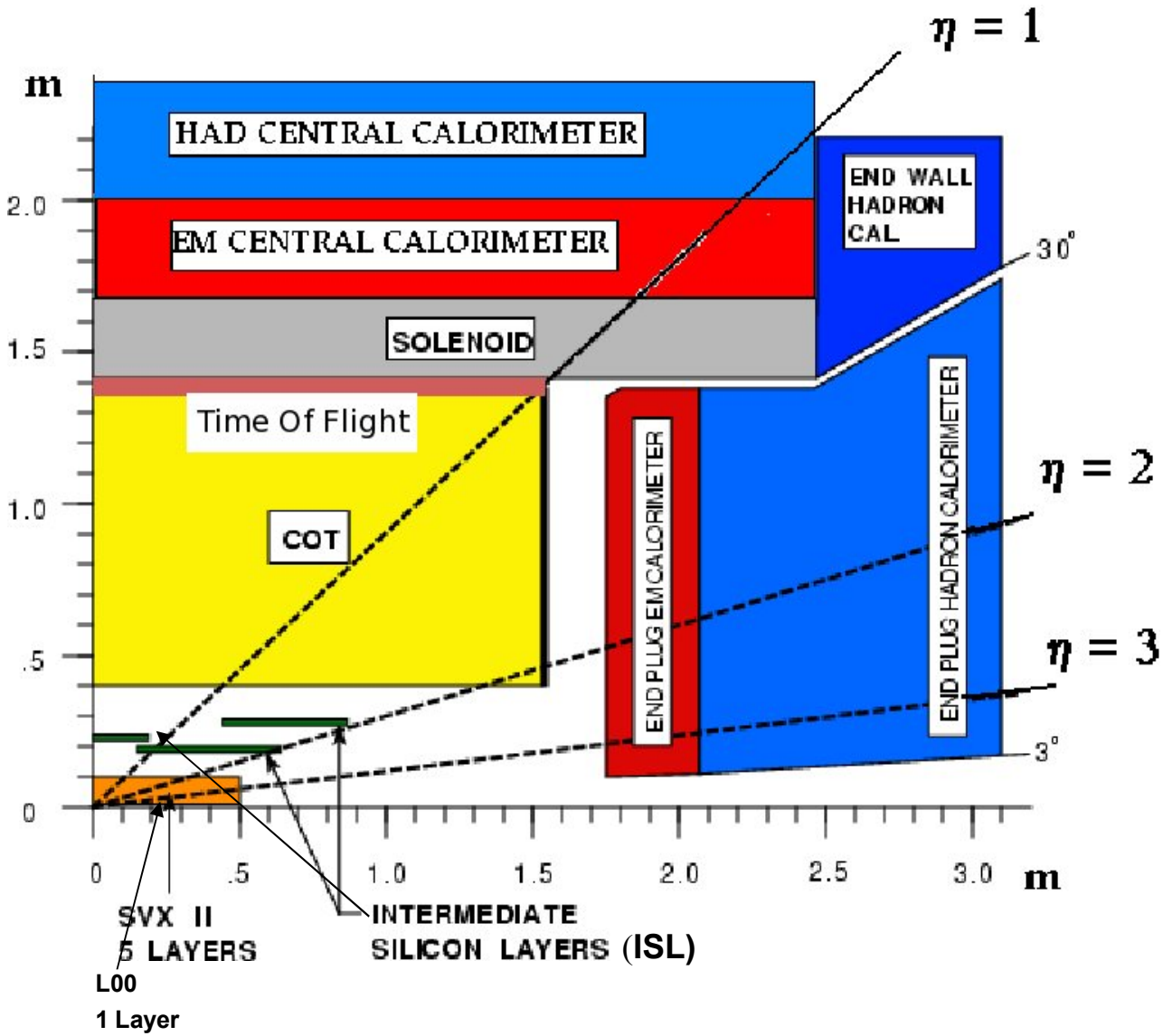

The CDFII Silicon detectors

OVERVIEW

L00: Single-sided strips: "Narrows" (SGS Thomson and 2 Microns)
"Wides" (Hamamatsu).

SVX: Double-sided strips: Layers 0,1,3 (Hamamatsu) perpendicular strips,
Layers 2,4 (Micron) small angled strips.

ISL: Double-sided strips: (Hamamatsu+Micron) small angled strips

All the sensors were silicon microstrips with barrel geometry,
no pixel, no forward disks.
In all the ladders the readout chip was the custom designed chip SVX3D.

The Silicon Detectors

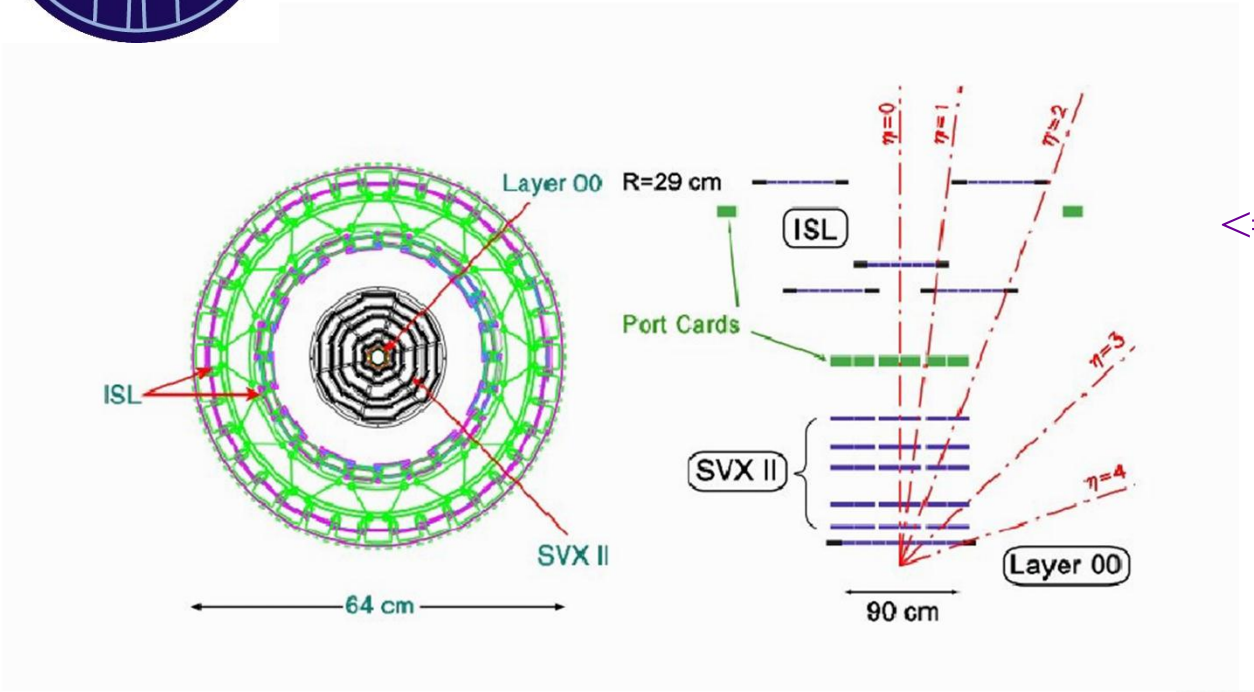

<== X-Y (r-phi) and Y-Z (r-z) views

L00 detail ==> narrow sensors

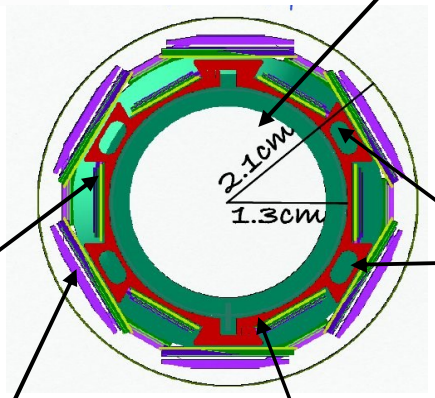

Beam pipe

Cooling lines

wide sensors

carbon support

The Silicon Detectors: SVXII

SVXII detail:
3 barrels
5 layers
12 wedges

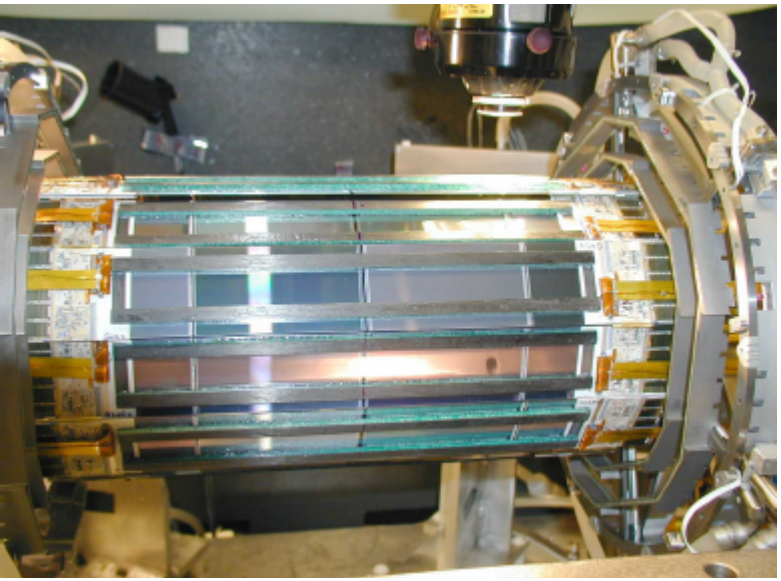

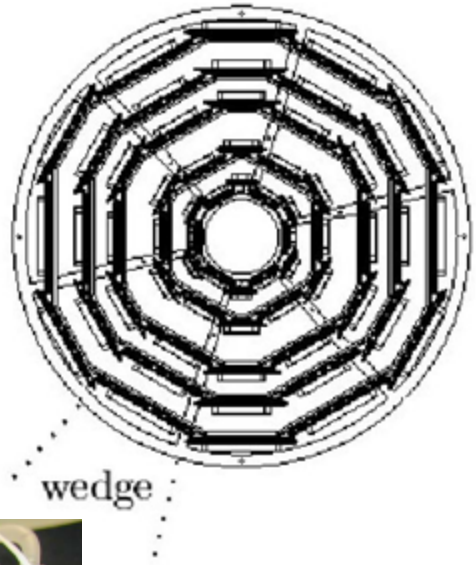

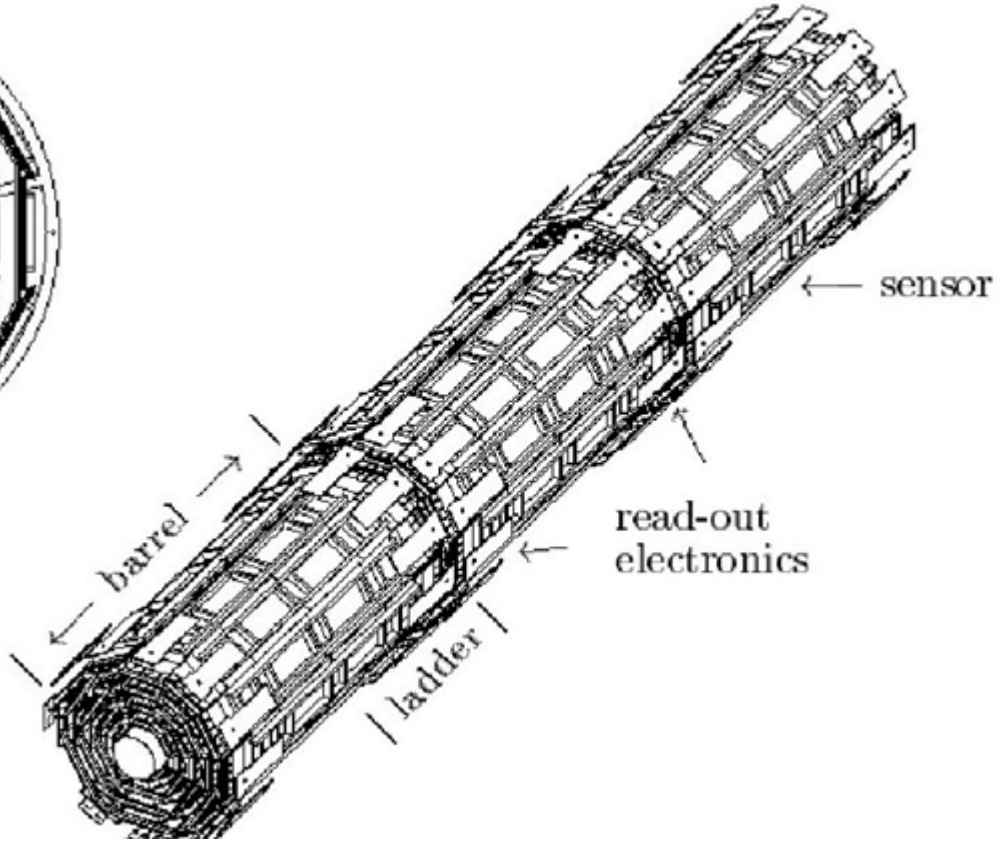

SVXII: the $R-\varphi$ readout is used directly in the trigger.

The Silicon Detectors: ISL

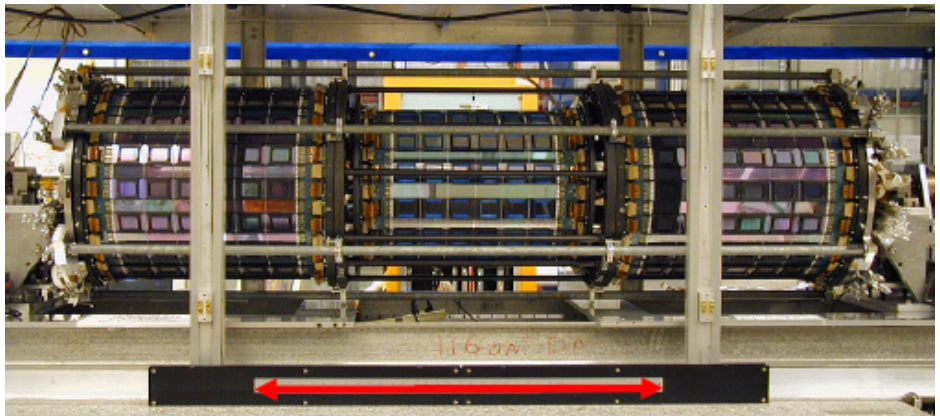

1 m

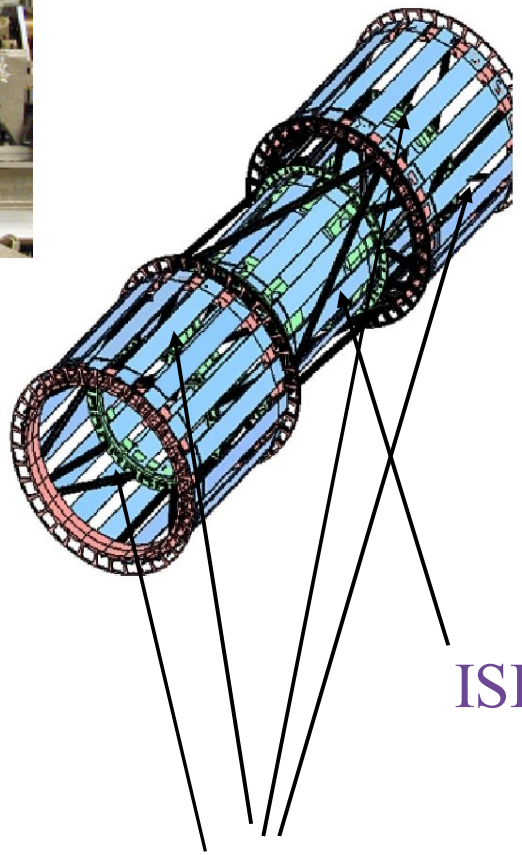

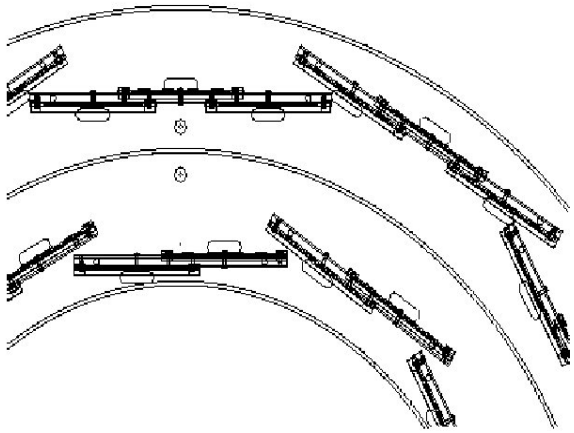

ISL central

ISLforward:
(inner and external barrels)

Radiation damage

- **Two general types of radiation damage to the sensors:**
  - **Crystal damage** due to Non-Ionizing Energy Loss (NIEL): displacement damage, crystal defects.
    - increase of shot noise, change of effective doping concentration, increase of charge carrier trapping.
  - **Surface damage** from Ionizing Energy Loss (IEL) causing accumulation of charge in the SiO2 and the Si/SiO2 interface.
    - Inter-strip capacitance , breakdown behavior etc.

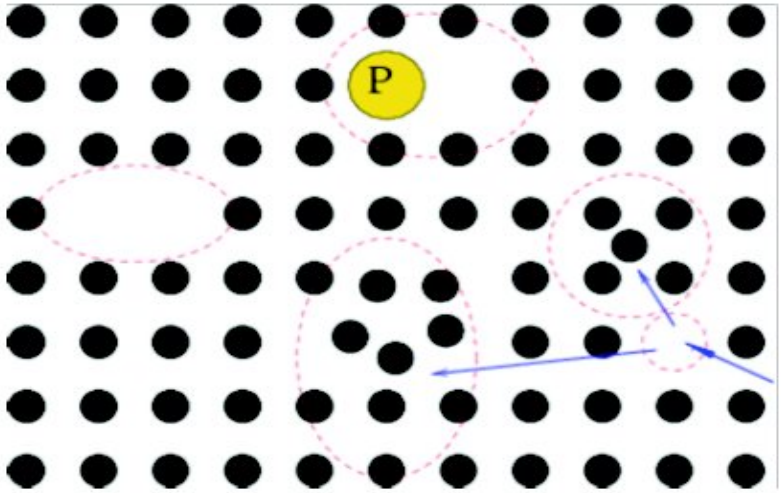

Crystal damage to the sensors is the main concern for detector longevity

Aging studies: variables of interest

Information on integrated radiation dose in a sensor is obtained by

- ✓ **evolution of bias current:** provides "direct" information on the crystal condition, due to increase in leakage current. Change in leakage current is linear with the absorbed dose $\Delta I_{leak} = \alpha \, \Delta \Phi_{eq}$, measured in 1-MeV neutron equivalent fluence [cm^{-2}] (α is the damage factor)
- ✓ **evolution of depletion voltage:** gives information on our ability to deplete the sensors in the future. Its extrapolation predicts the need to raise applied bias voltage and its limit.
- ✓ **Signal-over-noise (S/N) studies:** provide estimates of usability of the detector in charged particle tracking and in turn for physics analyses.

Evolution of bias current

Bias voltage (V)

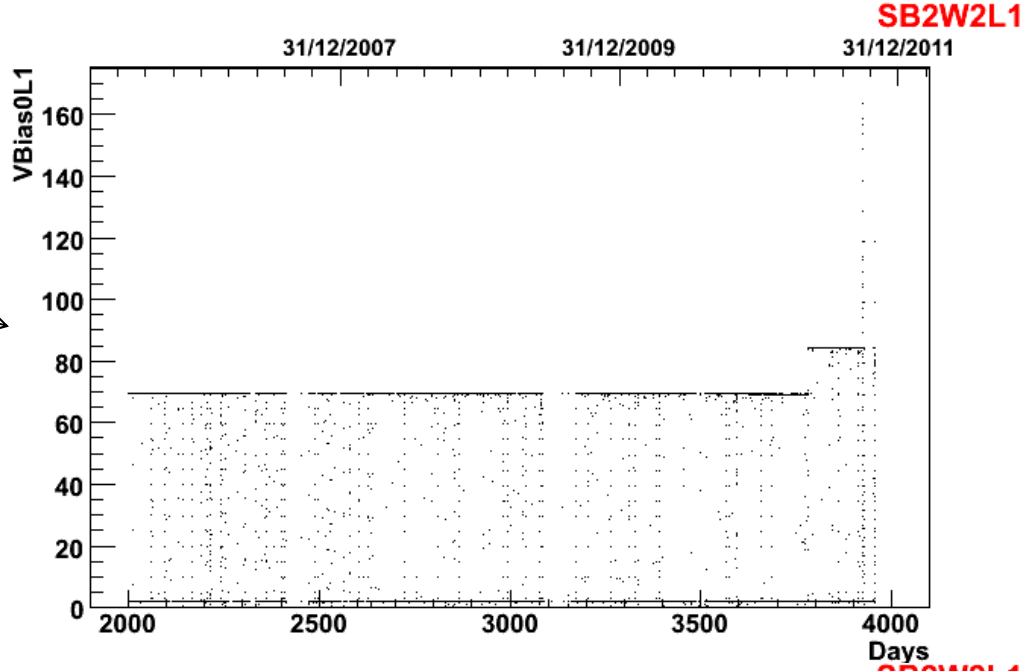

Expected behaviour of bias current in a silicon strip during data taking at fixed temperature:

Even if the bias voltage is constant the current increase due to radiation damage

Bias current (μA)

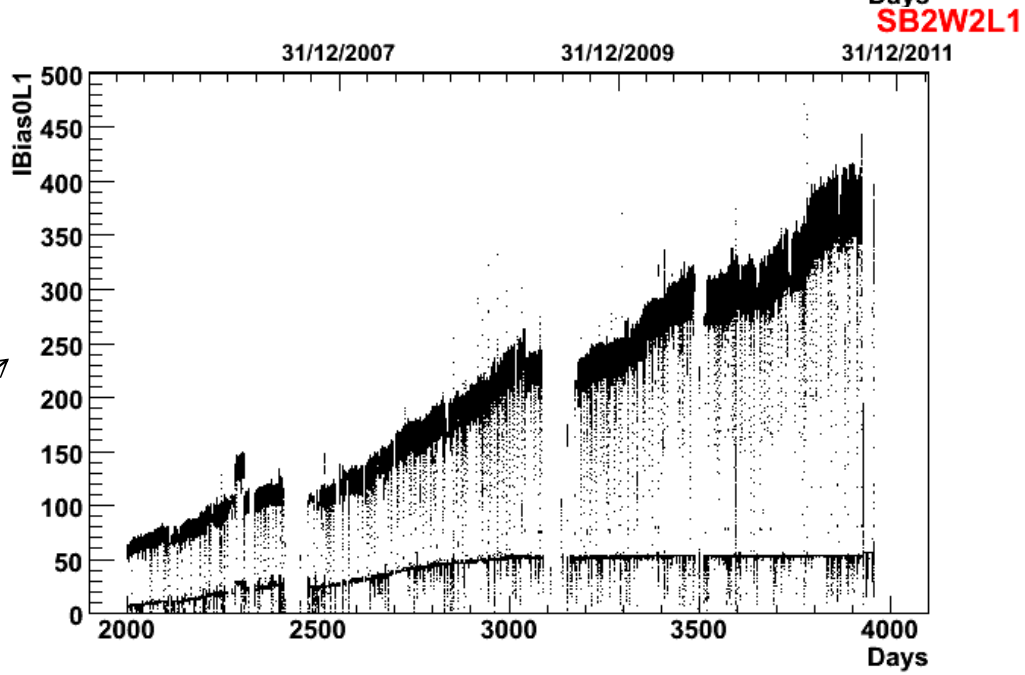

Depletion Voltage

Depletion voltage is the bias voltage required to get rid of free carriers in the bulk of the detector.

The expected evolution depends on the dose (Hamburg Model):

Before type inversion the depletion voltage decreases due to the reduction in the amount of free carriers

After type inversion, depletion voltage steadily increases.

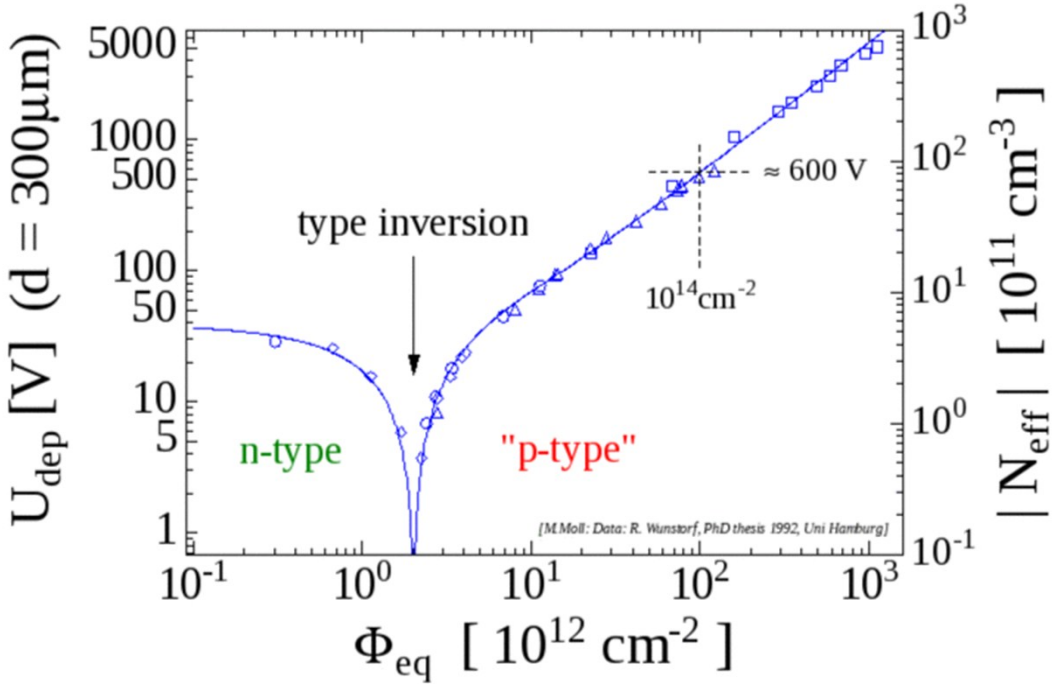

R. Wunstorf, Ph.D thesis, Hamburg University (1992)

Sensor can operate while the Bias Voltage is below the Breaking Voltage

Depletion Voltage evolution

$$V_{dep} \sim |N_{eff}|\, d^2$$

Parametrization of the variation of ΔN_{eff}

Effective doping concentration of "n"-type silicon

$$\Delta N_{eff}(\Phi, t, T) = \Delta N_C(\Phi) + \Delta N_Y(\Phi, t, T)$$

Two mechanisms: Donor Removal and Acceptor Creation

Increases with Φ (time independent)

"Reverse Annealing", (increases with Φ, time and Temperature)

$$\Delta N_C(\Phi) = N_{C0}(1-e^{-c\Phi}) + g_C\Phi, \quad \Delta N_Y(\Phi, t, T) = g_Y\Phi\left[1 - 1/(1+t/\tau_Y(T))\right]$$

See: RD50 Collaboration http://rd50.web.cern.ch/rd50

Depletion voltage Measurement

From charge (signal) collection efficiency:

- Charge collection is proportional to the depleted volume.
- Fully depleted sensor ➔ charge collection efficiency saturates.
- Extracted track residual information.
- Can be performed on single sided and double sided microstrips.
- This measurement is beam-time consuming.

From the noise at the n-side:

- Thermal noise from free carriers on the n-side is reduced with depletion (on the p-side)
- Is possible only on double sided microstrips before the inversion.
- This measurement is not beam-time consuming

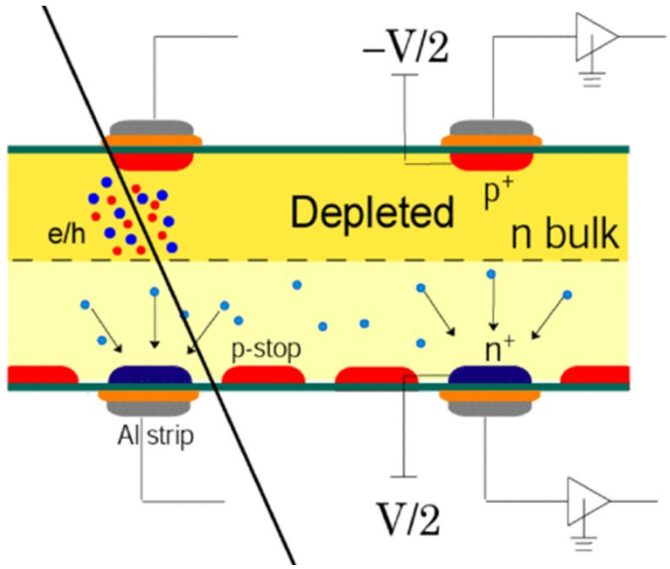

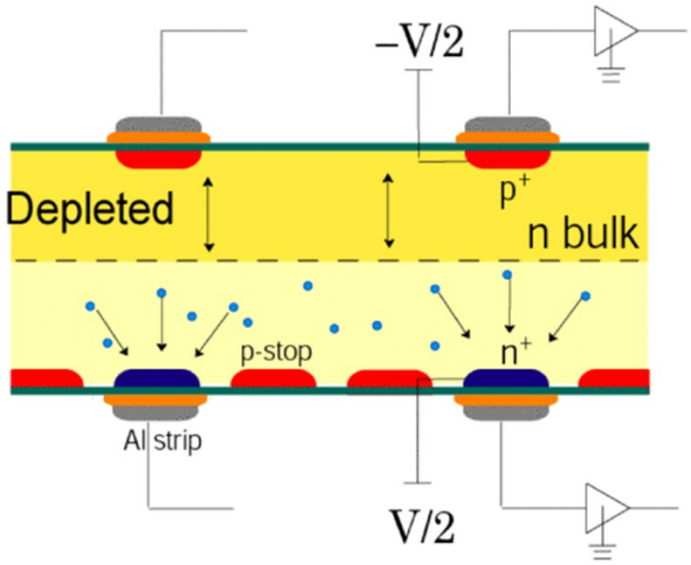

Depletion Voltage study – Signal Vs. Bias

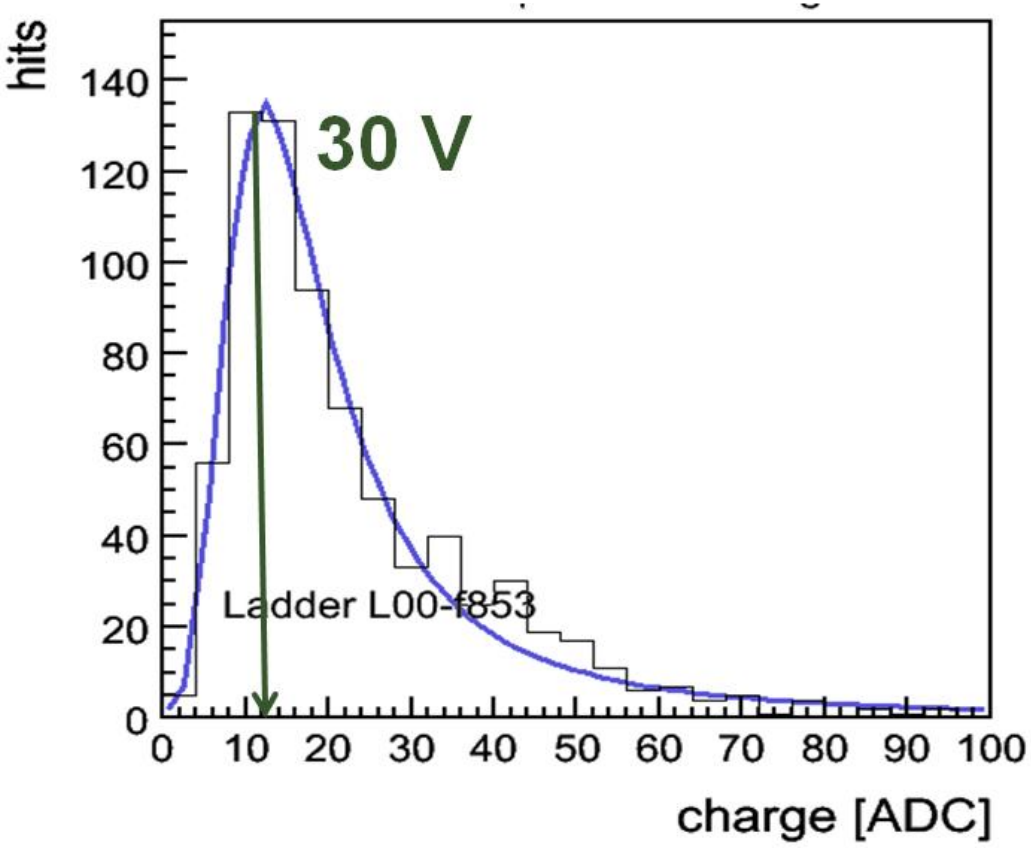

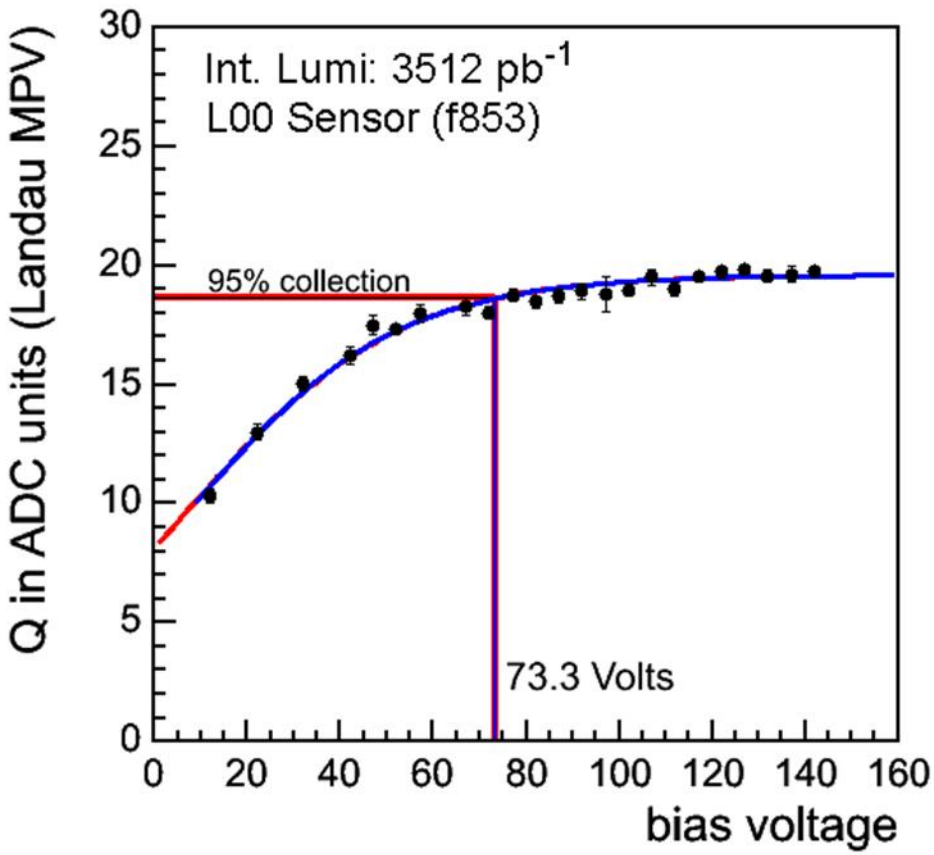

Depletion Voltage study: Signal Vs. Bias Voltage

- Plot charge collected for different bias voltages
- CDF defines depletion voltage, V_d, as the minimum voltage that collects 95% of the charge at the plateau

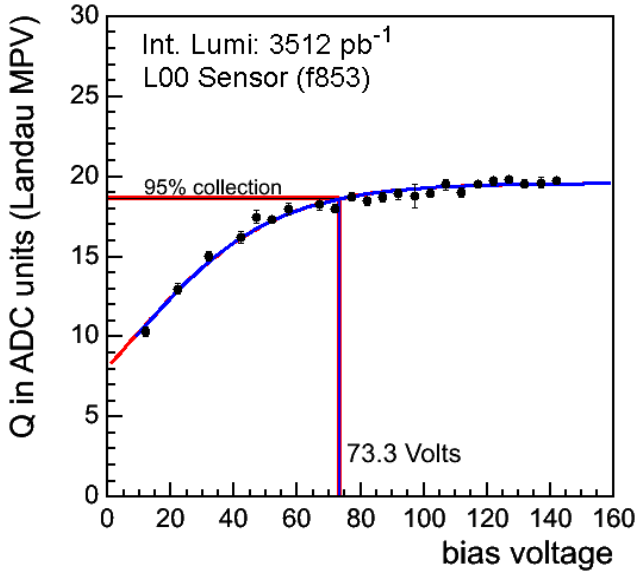

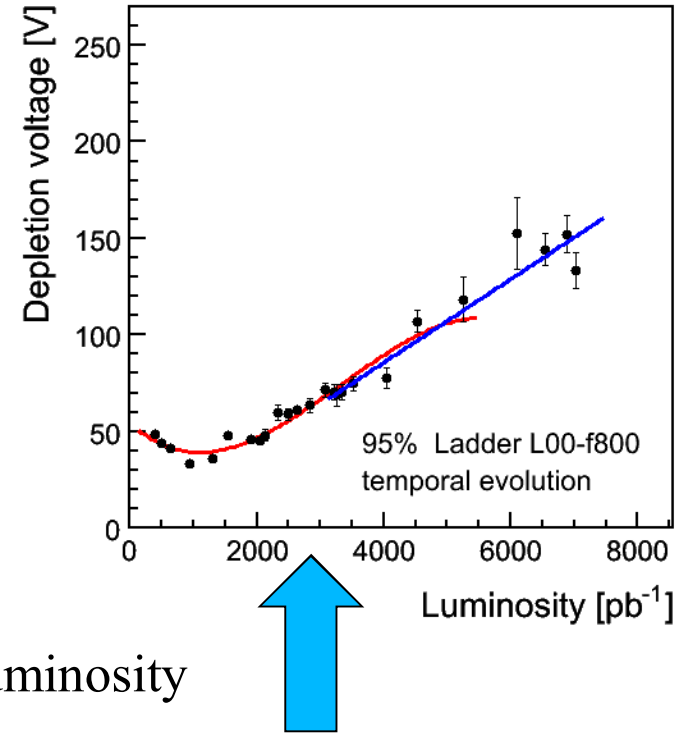

- Depletion Voltage as a function of integrated luminosity

3rd order polynomial fit around the inversion point Linear fit to extrapolate to the future

More details in R. Ballarin Ph.D. thesis:
http://lss.fnal.gov/archive/thesis/fermilab-thesis-2011-28.shtml

Depletion Voltage evolution observed in L00 and SVX-L0

Preliminary results for L00

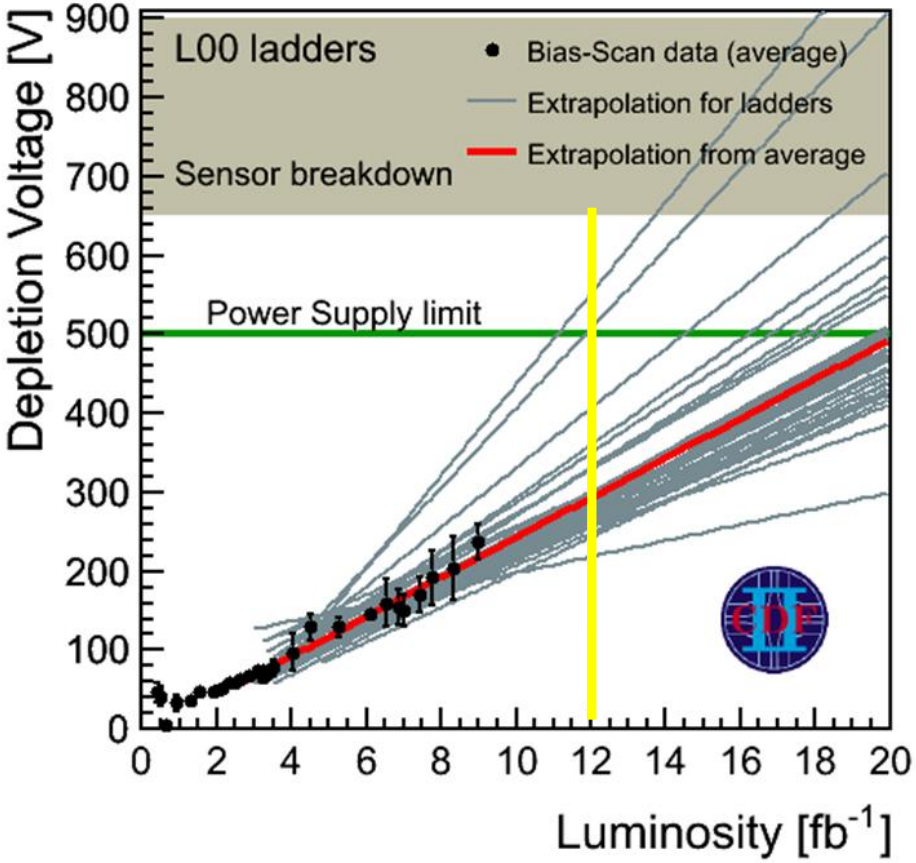

Preliminary results for SVX-L0

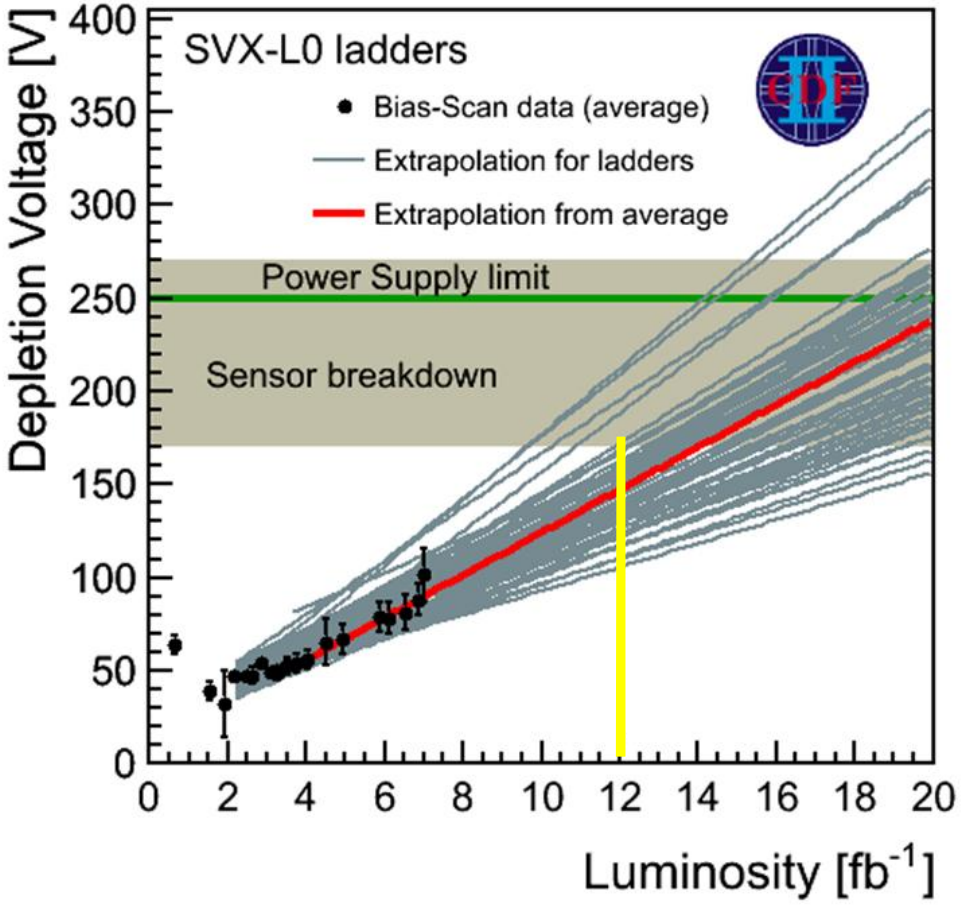

Preliminary result on L00:

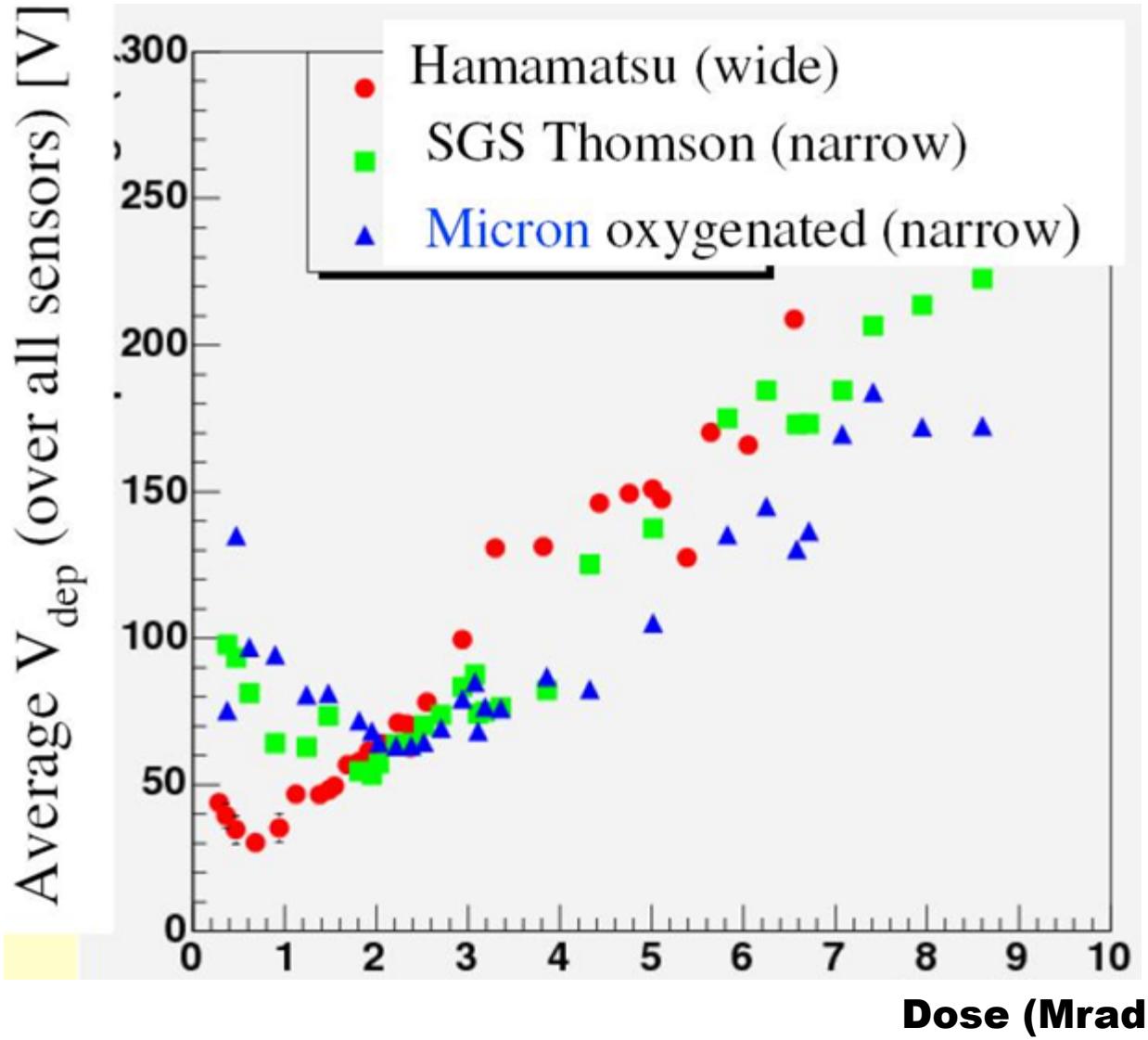

We are trying to see the behavior of different vendors: Studies still ongoing

Signal / Noise projection

Signal from J/ψ → $\mu^+\mu^-$ tracks strip cluster charge,
Noise estimation from regular calibrations

r-phi

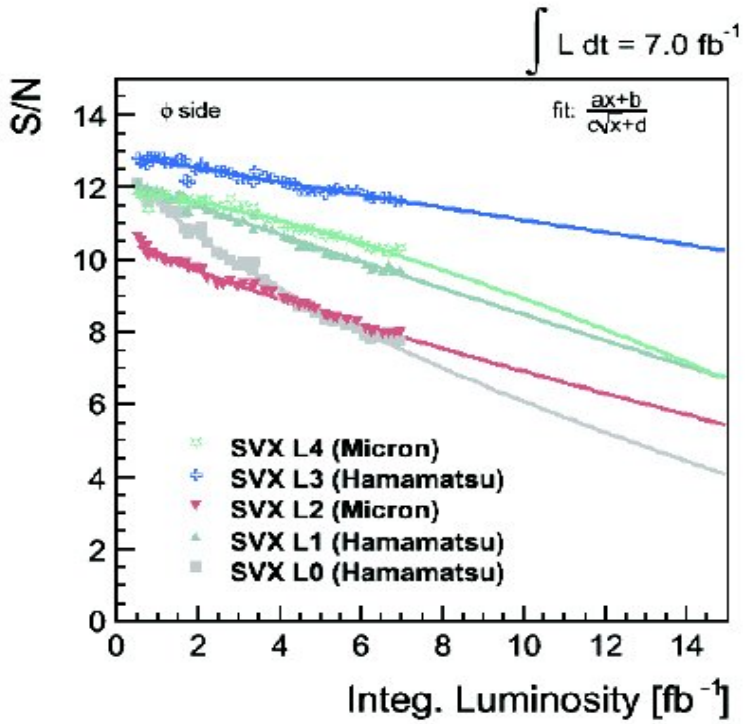

L00

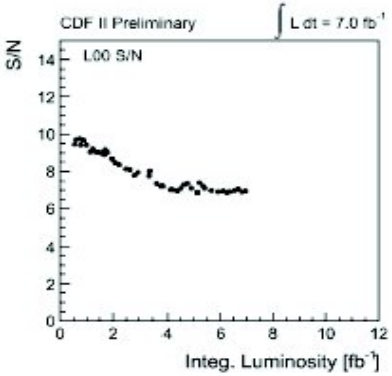

z

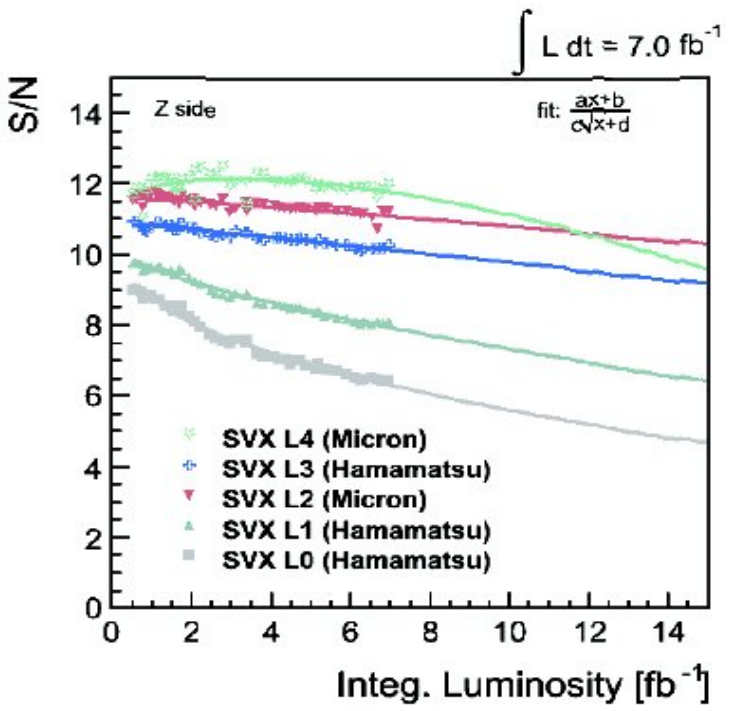

Not only the sensors are in a radiation environment

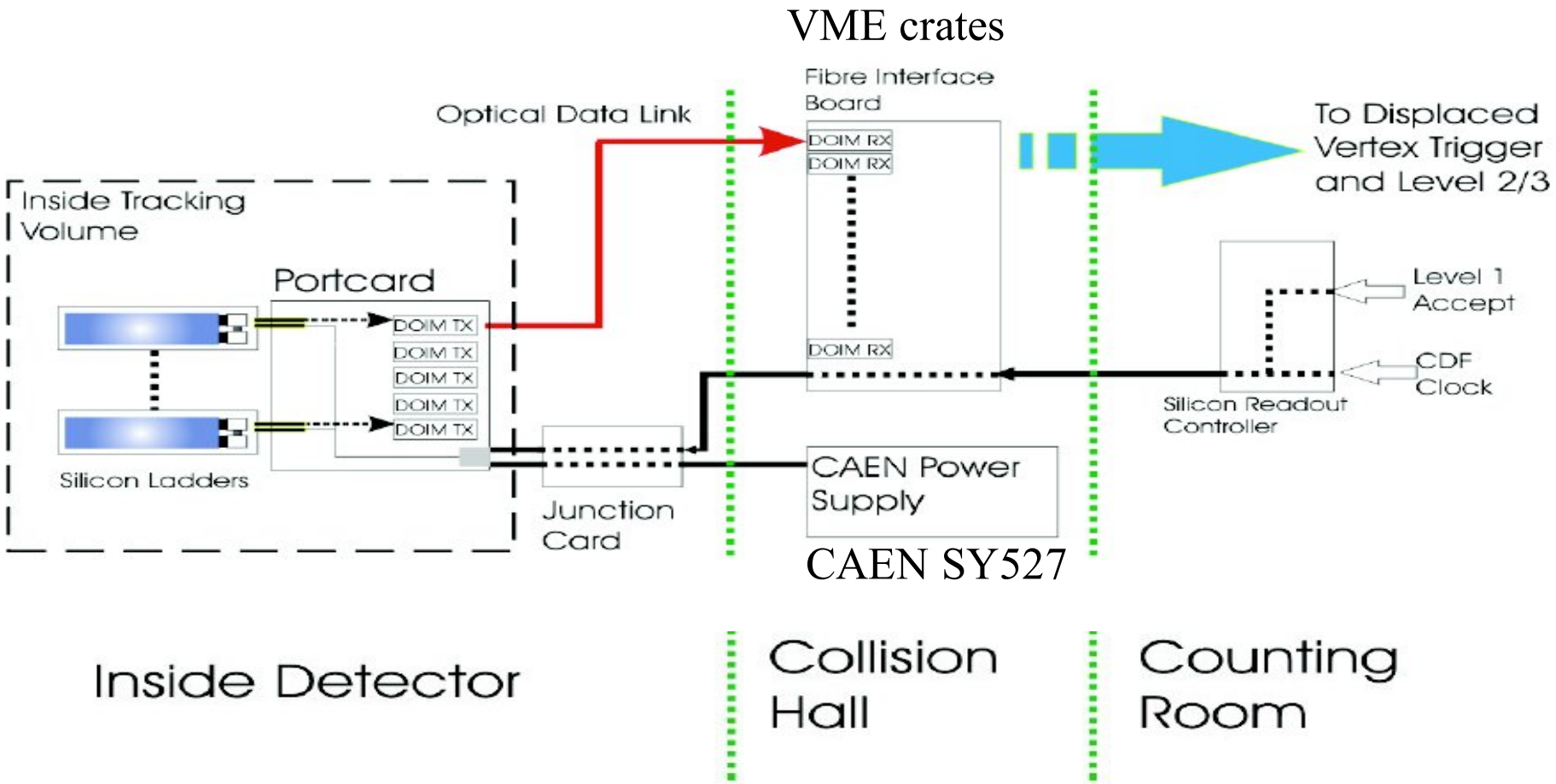

- **SEU requires FPGA and fuse replacement on FIBS (~2/year)**
- **Power Supplies need replacement capacitors every ~4 years**
- **DOIM TX light output decreases linearly with radiation dose**

Radiation Field inside the detector

Measured using ~1000 thermo-luminescent dosimeters (TLDs)

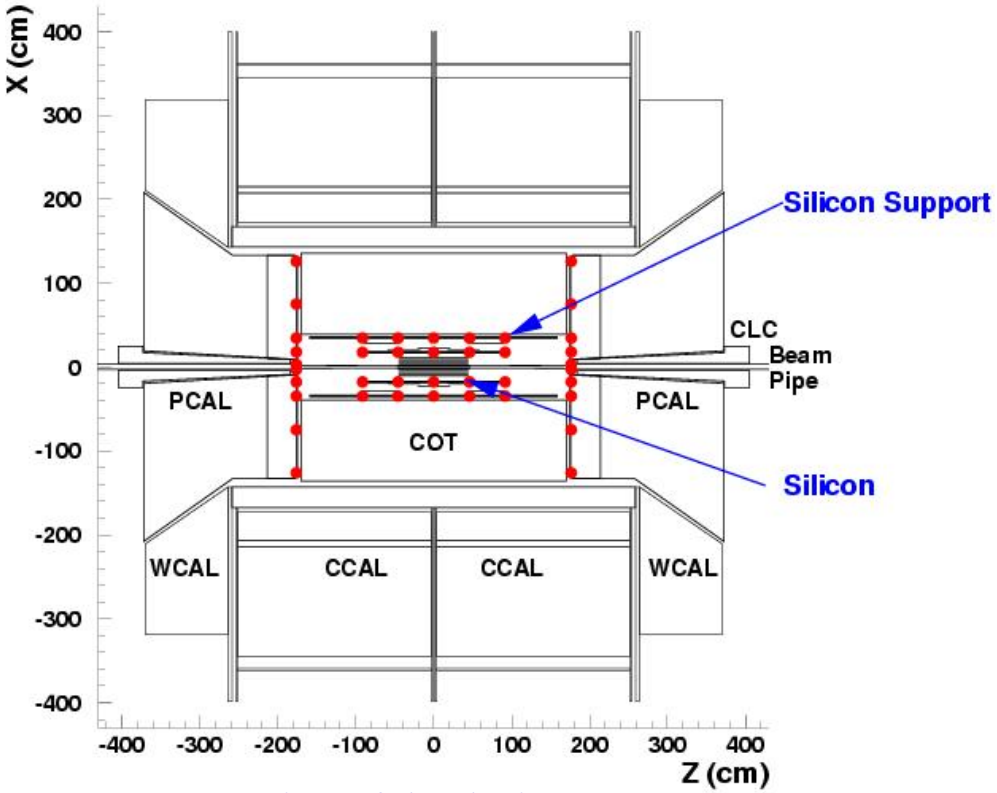

Location of the dosimeters

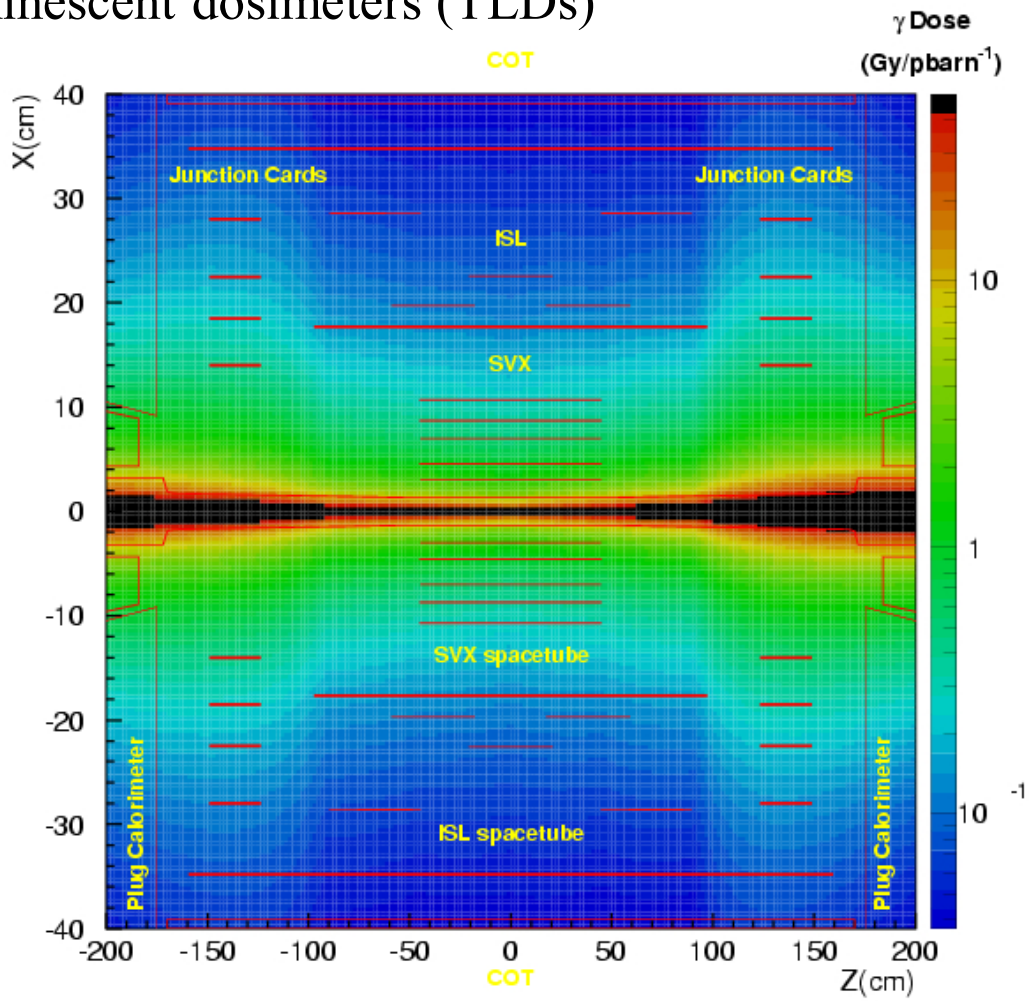

See:R.J. Tesarek *et al.*,
"A Measurement of the Radiation Environment in the CDF Tracking Volume",
Proceedings RESMDD02 conference, 10-13 July 2002, Florence, ITALY
See also:http://cdf-radmon.fnal.gov

The radiation intensity change during the collider operation: dose rate during beam injection and data taking

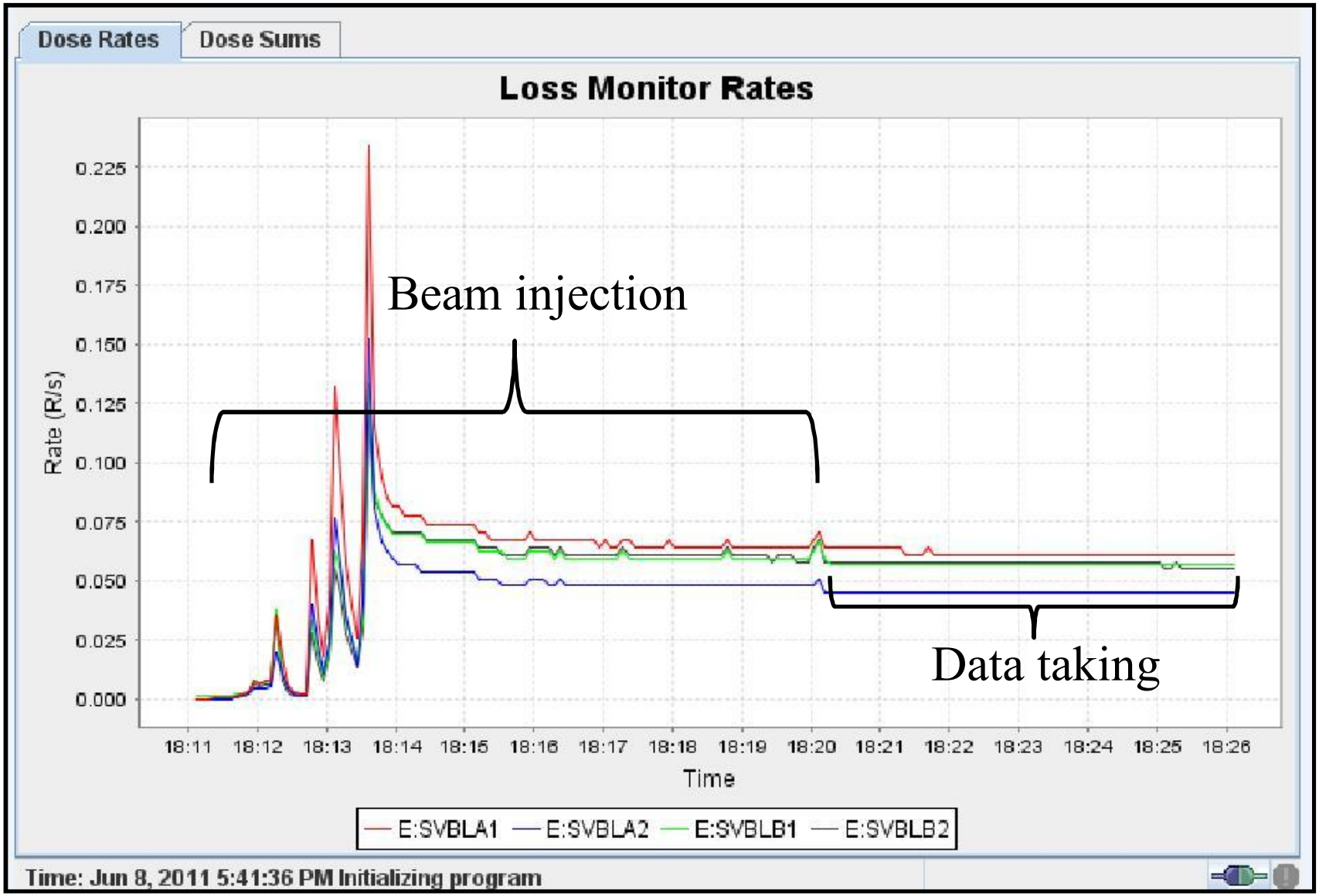

Beam dose during beam injection and data taking

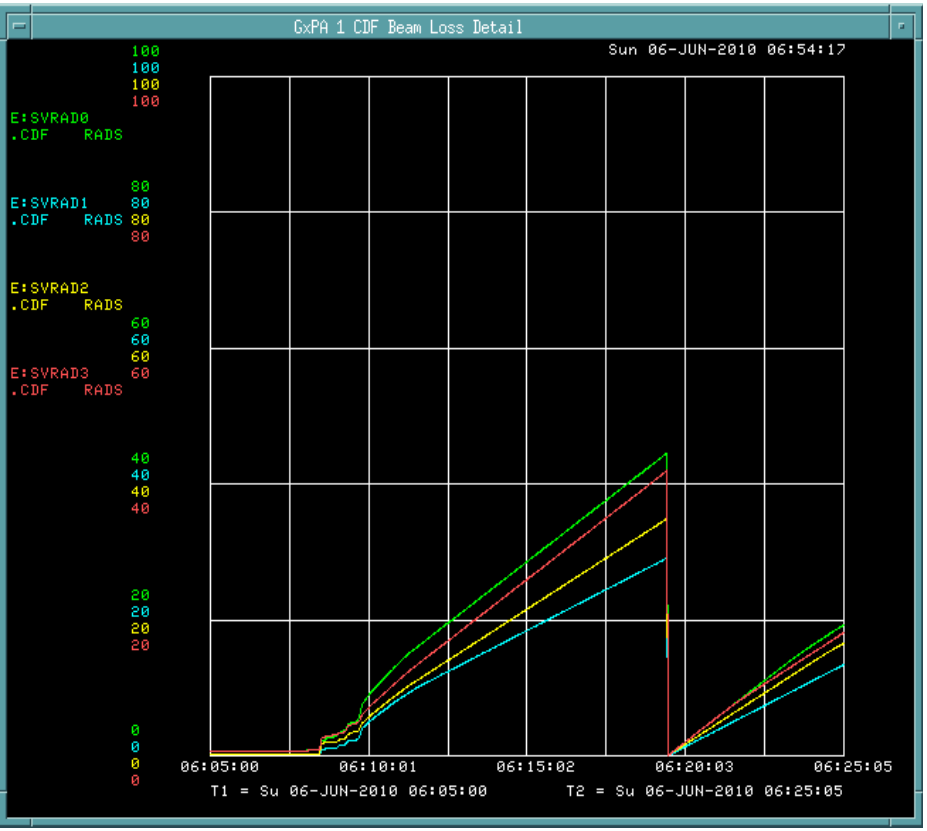

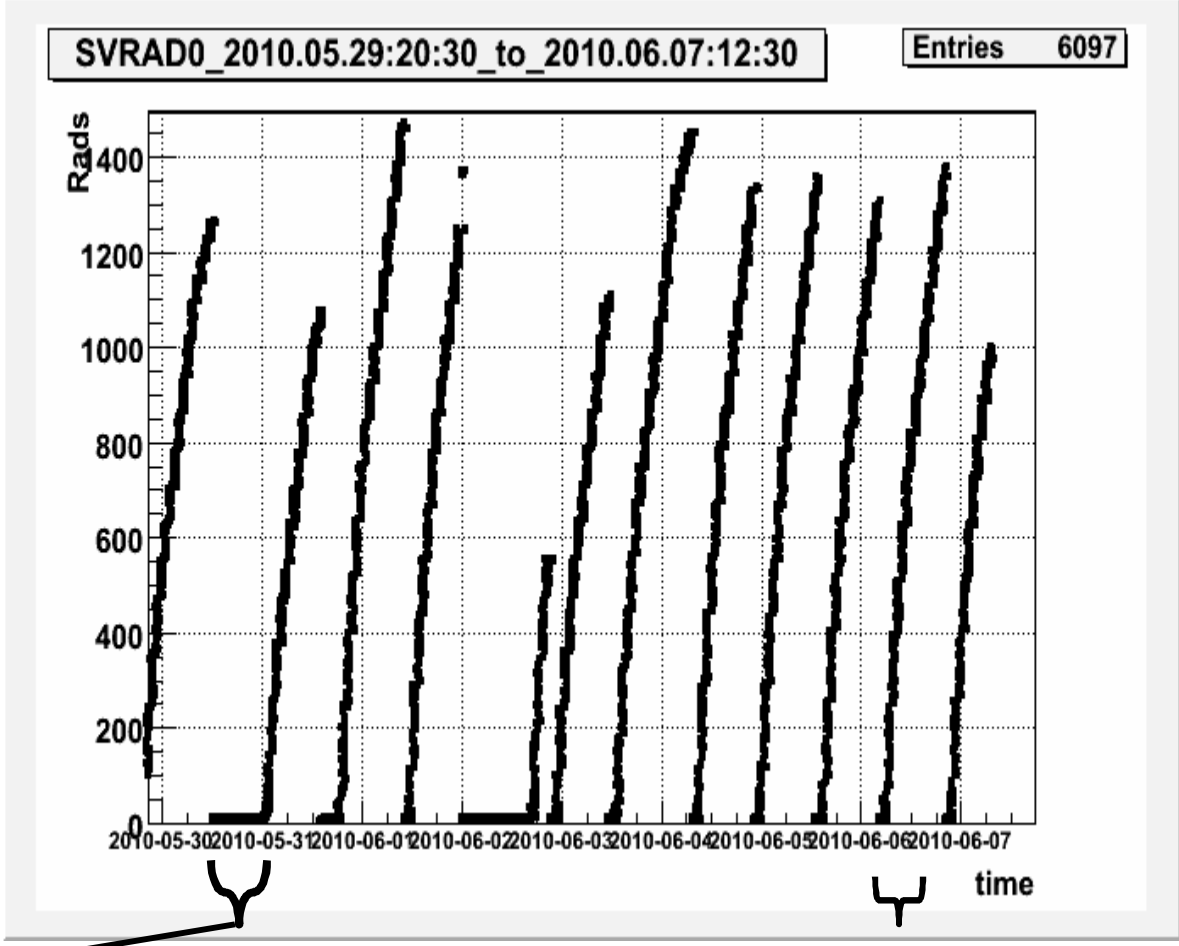

beam injection

Data taking

Beam losses

abort gap losses

beams losses

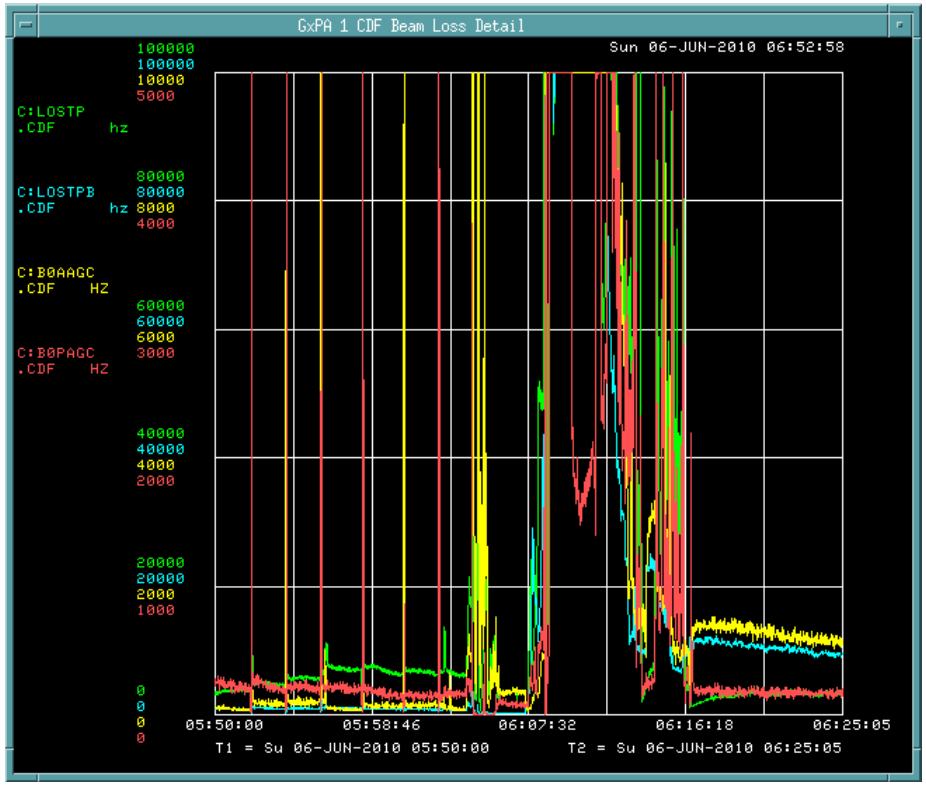

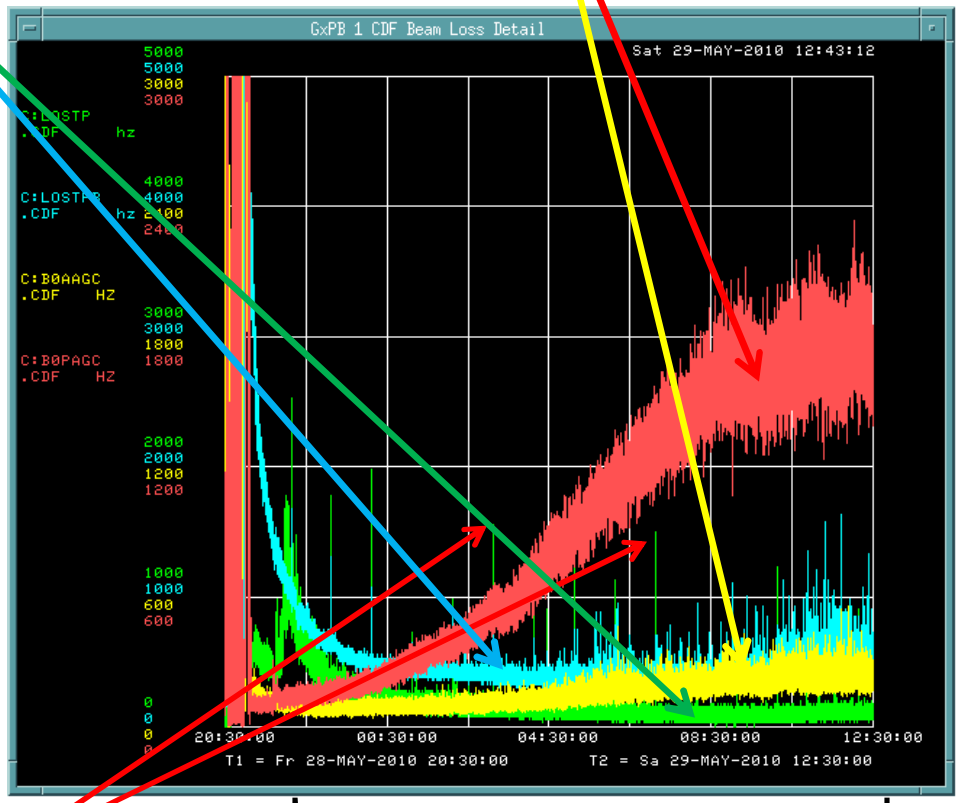

Beam intensity measurement (fly wire scans)

beam injection

data taking

Dose rate during beam dump

Clean abort

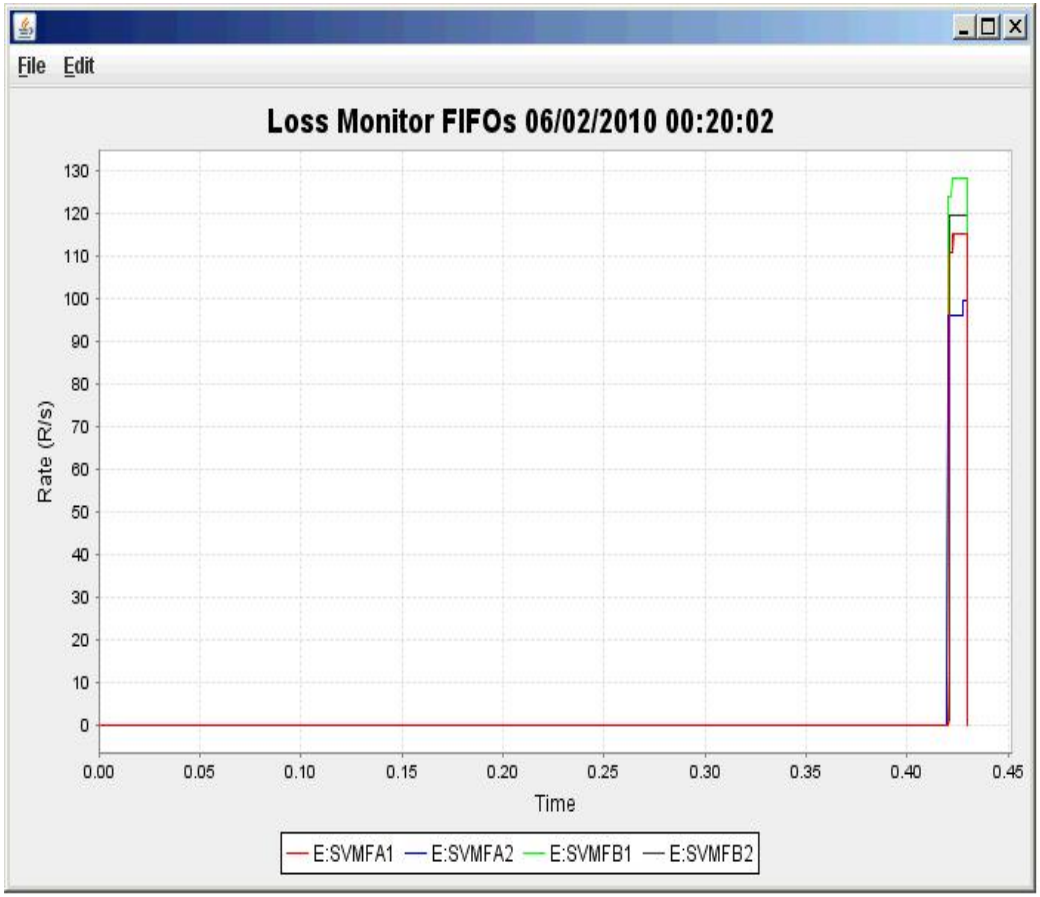

Quench

The annealing

This is what happens to the bias current stopping the irradiation and increasing the temperature: test beam studies shows that the bias current start to decrease for a fixed bias voltage.

R. Wunstorf, Ph.D thesis
Hamburg University 1992

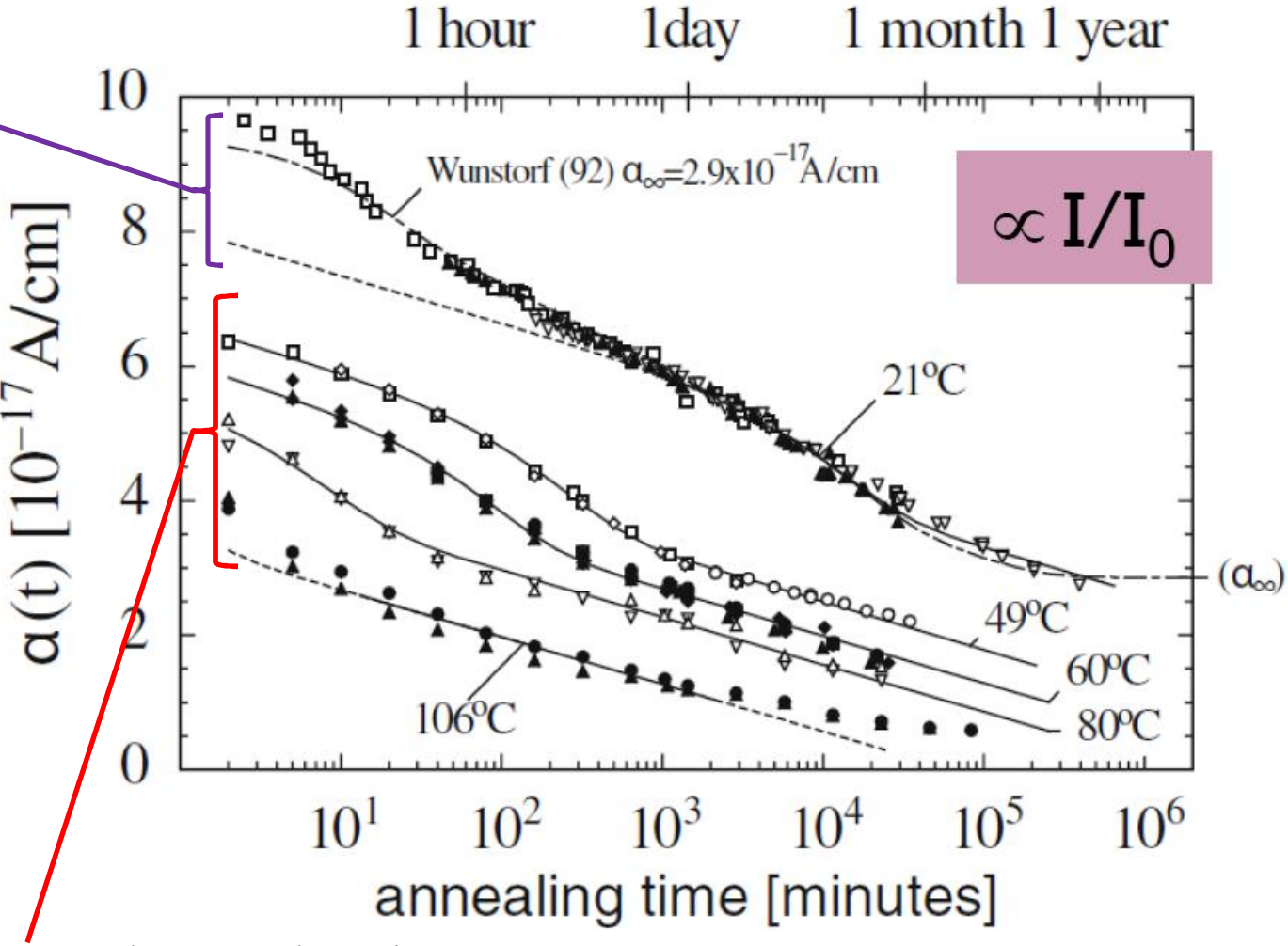

M.Moll (RD50 Coll.) Ph.D. thesis, Hamburg University 1999
https://mmoll.web.cern.ch/mmoll/thesis/pdf/moll-thesis.pdf

The annealing: effects on the Depletion Voltage

M.Moll *et al*, NIMA **439,** 282-292 (2000)

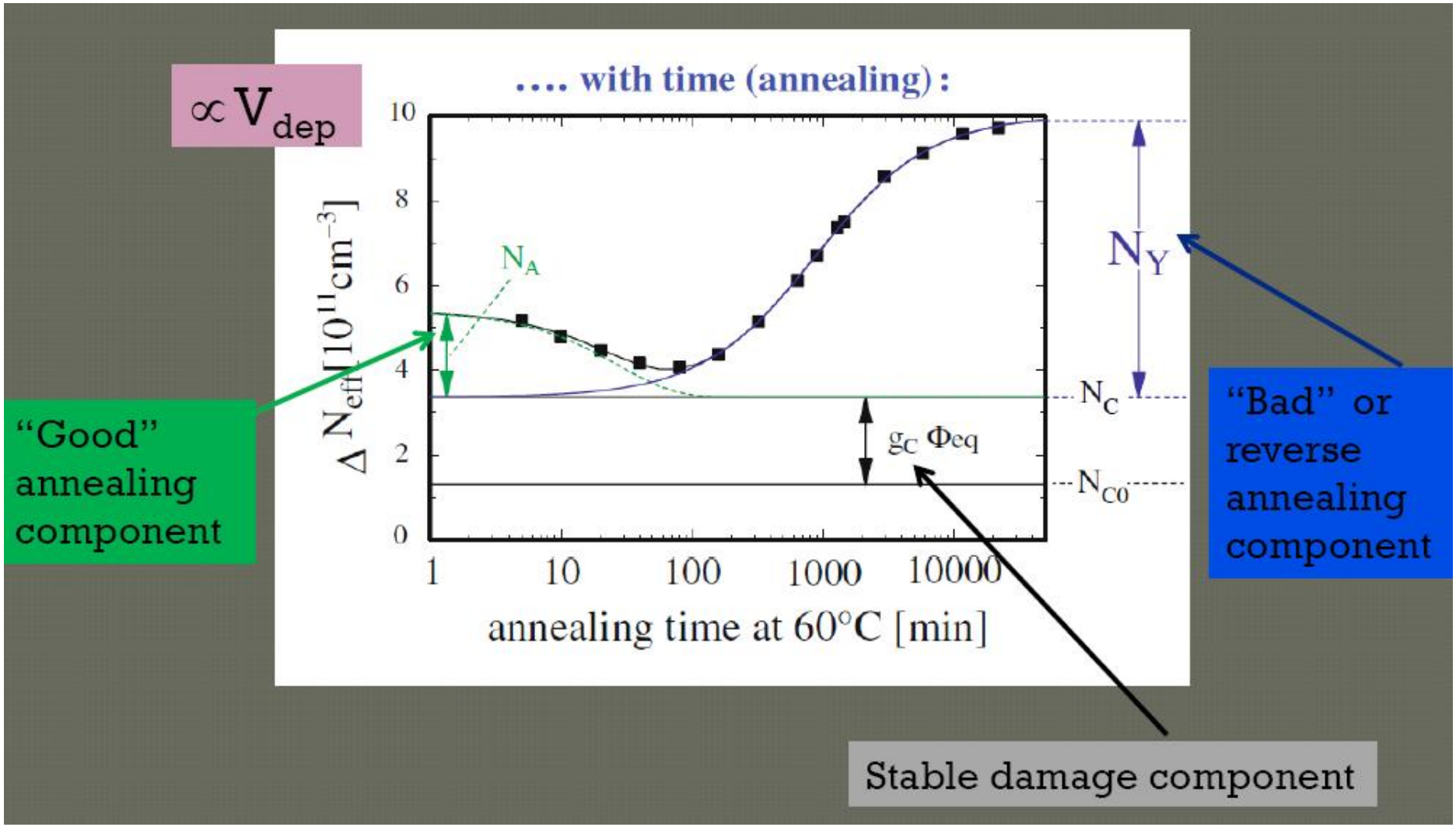

Preliminary results in CDF:

Operative temperature: -5 degree Celsius

Measurement Temperature: +18 degree Celsius, Vbias = fixed

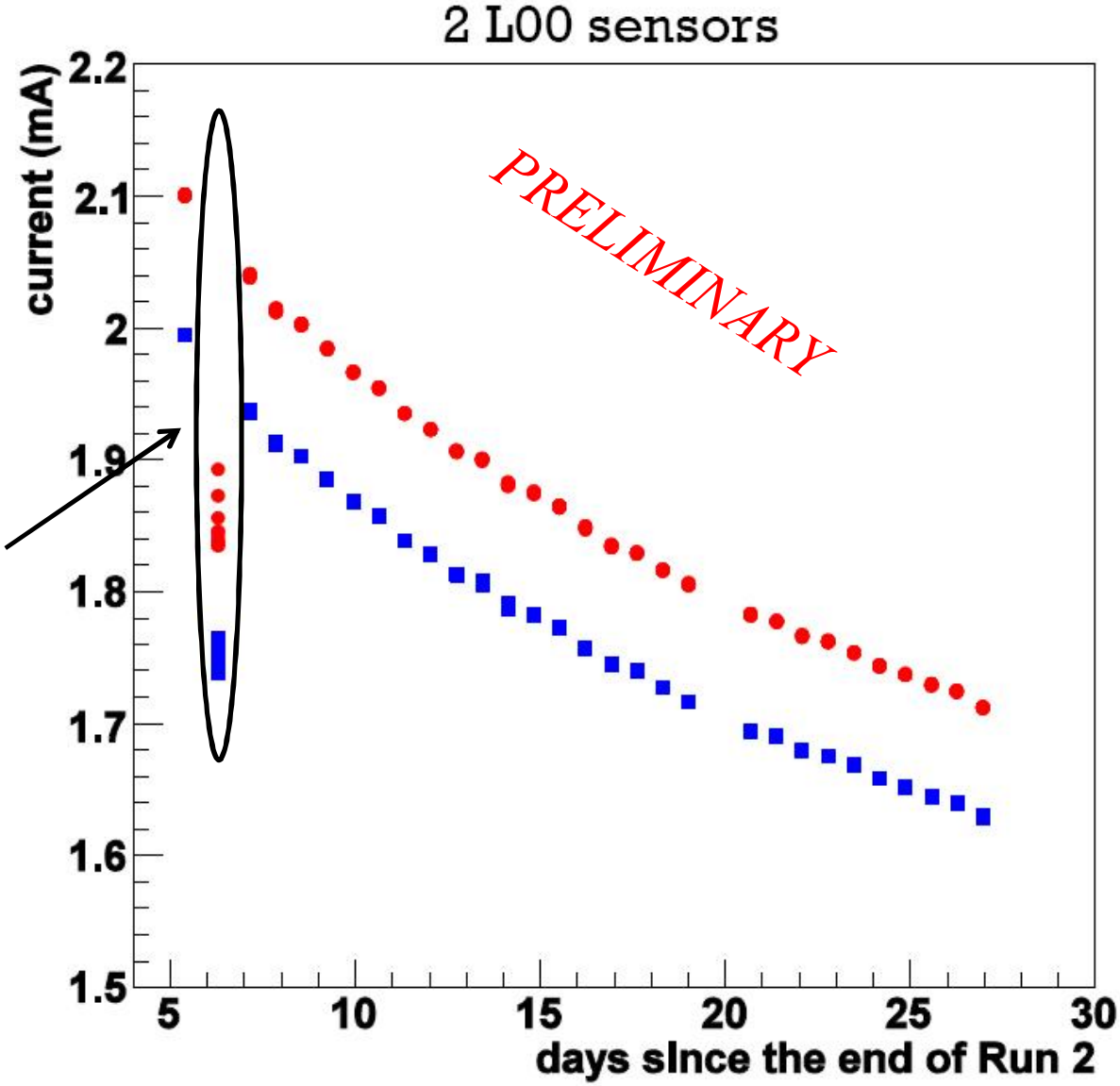

cooling system trip

Preliminary results

Operative temperatute: -5 degree Celsius
Measurement temperature +18 degree Celsius, Vbias =fixed

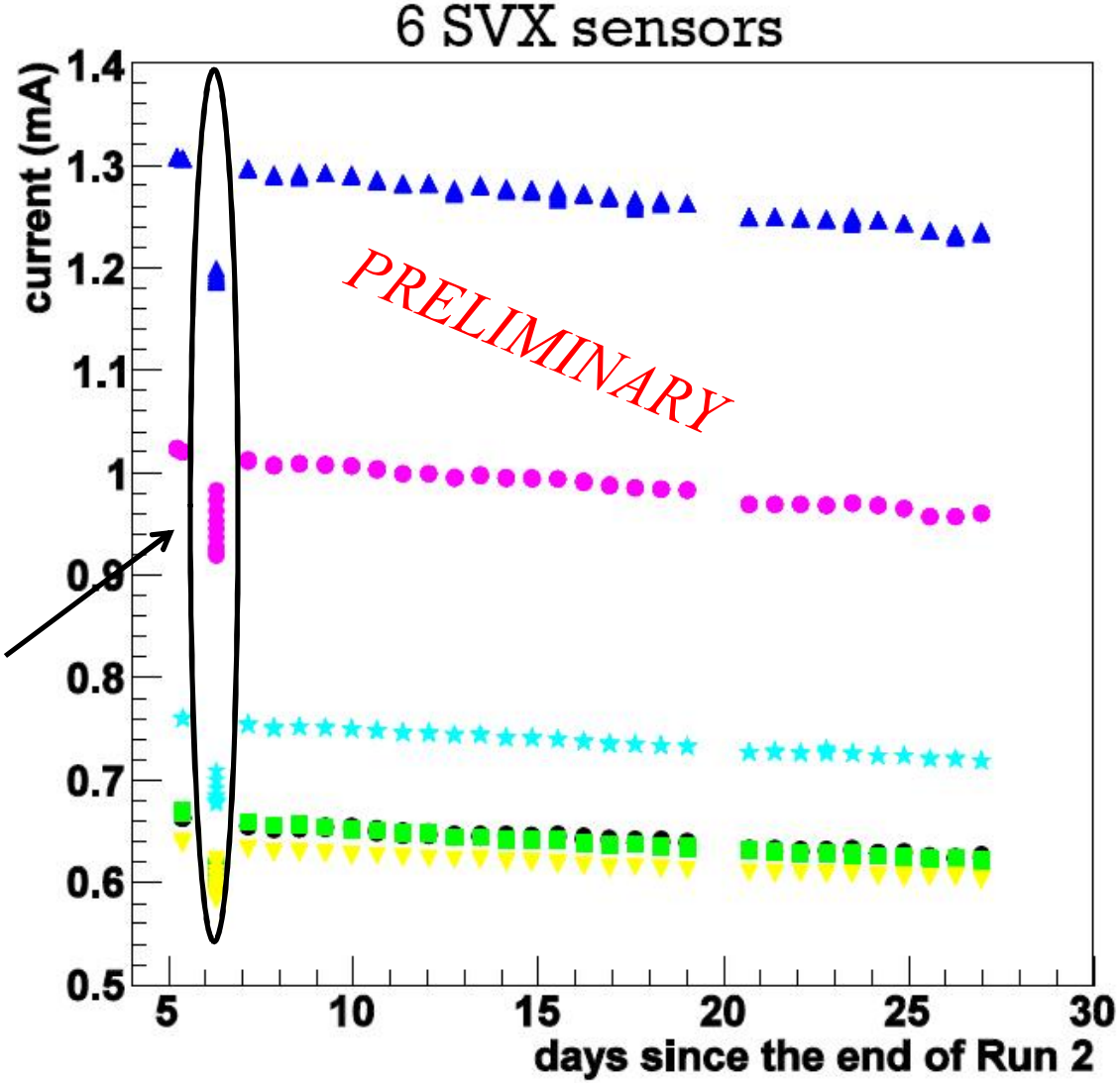

cooling system trip

Problems induced by trigger rates:

Wirebond Resonances

- Observed loss of data & power to *z* sides of ladders
  - Found to correlate with high trigger rates
- Failure due to wirebond resonances
  - Wires orthogonal to magnetic field
  - Wires feels Lorentz force during readout
  - If frequency is right, wires resonate and break

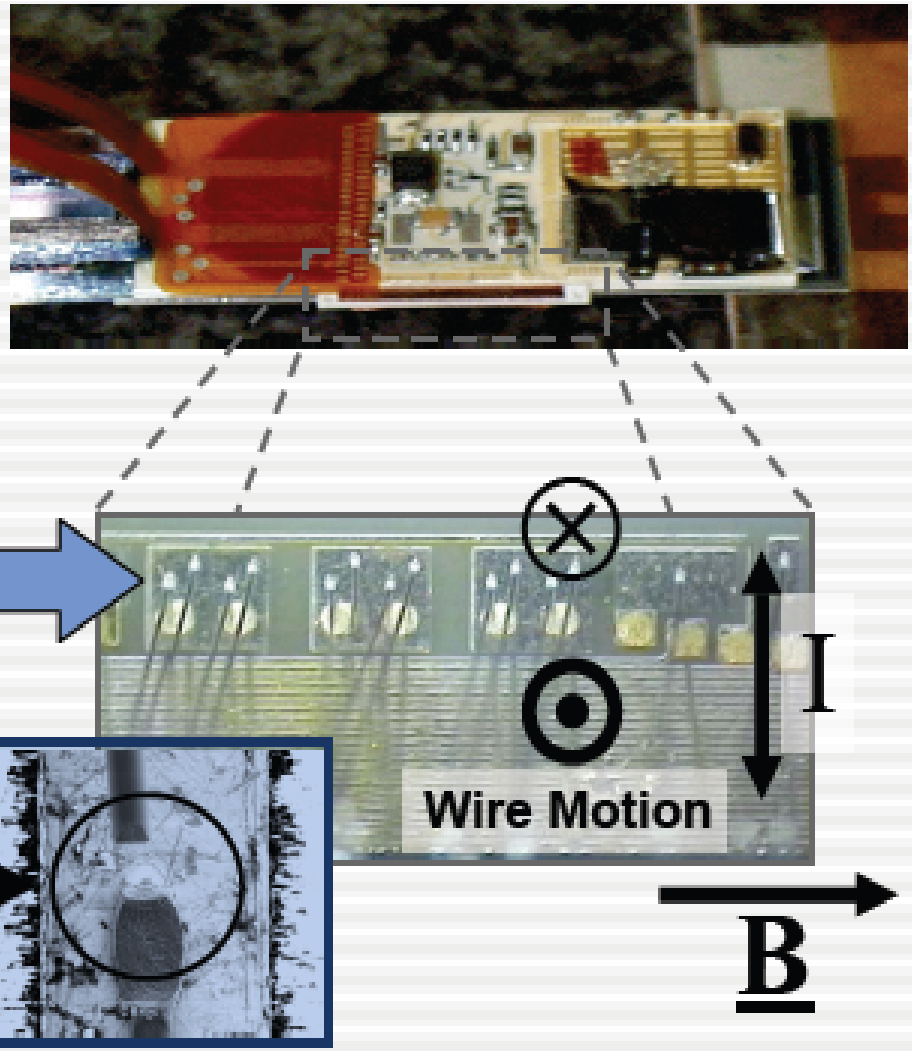

See: Gino Bolla *et al.*
http://www-cdf.fnal.gov/upgrades/silicon/TASK-Force/line3/line3.html

Effect of the readout chips heating

In SVXII the readout chip is in touch with the cooling line, the sensor is not cooled directly: simply switch ON/OFF the chips the bias current in the ladder change a lot.

IV Scans

Bias current (μA)

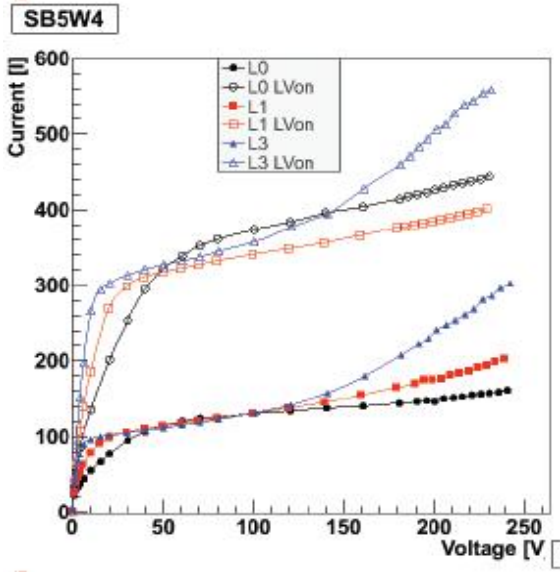

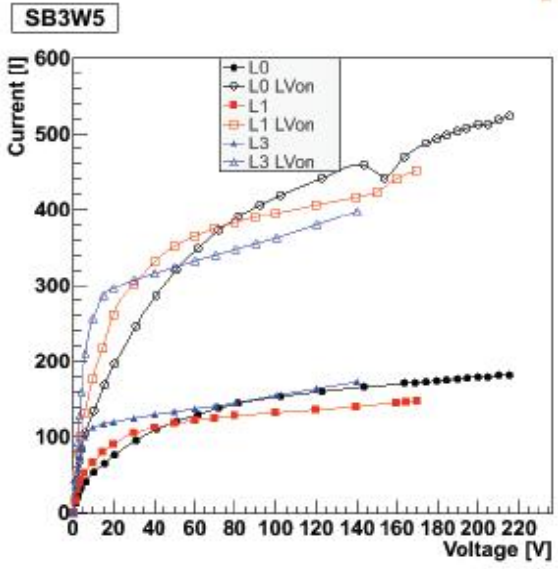

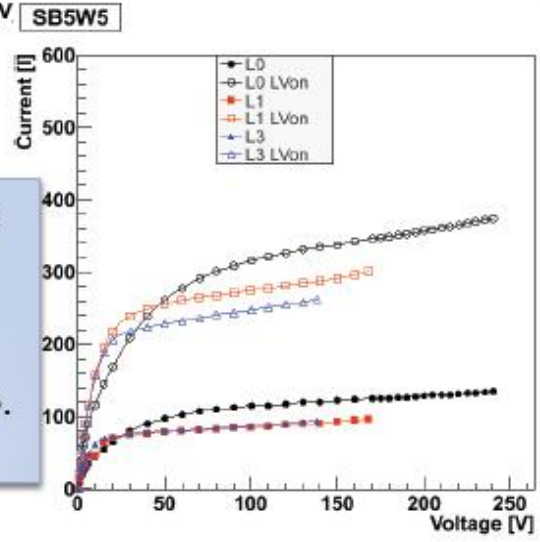

- Outer sensors are larger and are read out using more chips.
- LVon and LVoff cases are different due to temp. effect.

Effect of the readout chips heating

This effect was not observed in L00 ladders where the sensor itself is cooled and the chip is far from the sensor.

Bias current (μA)

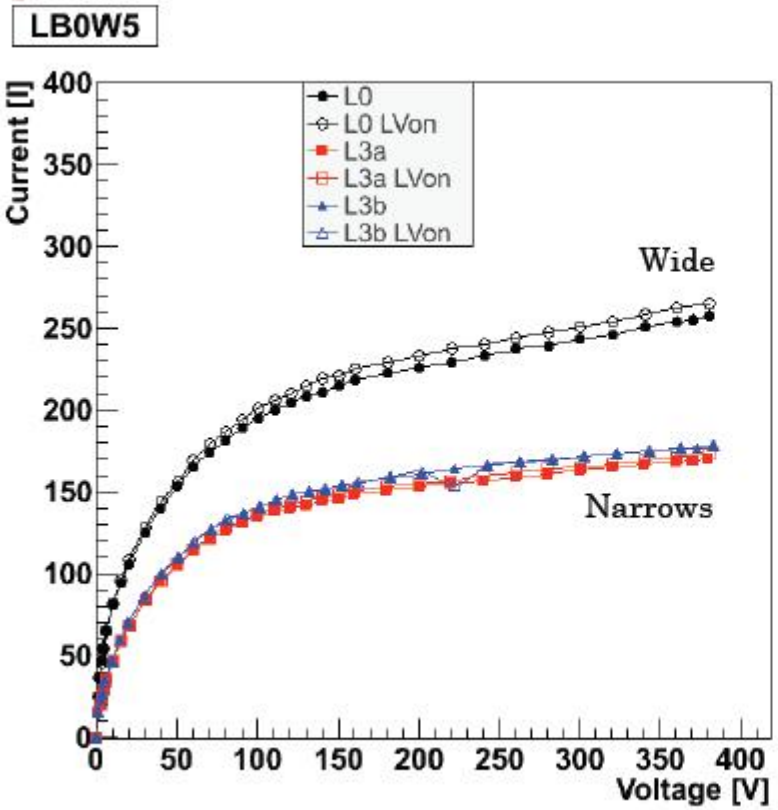

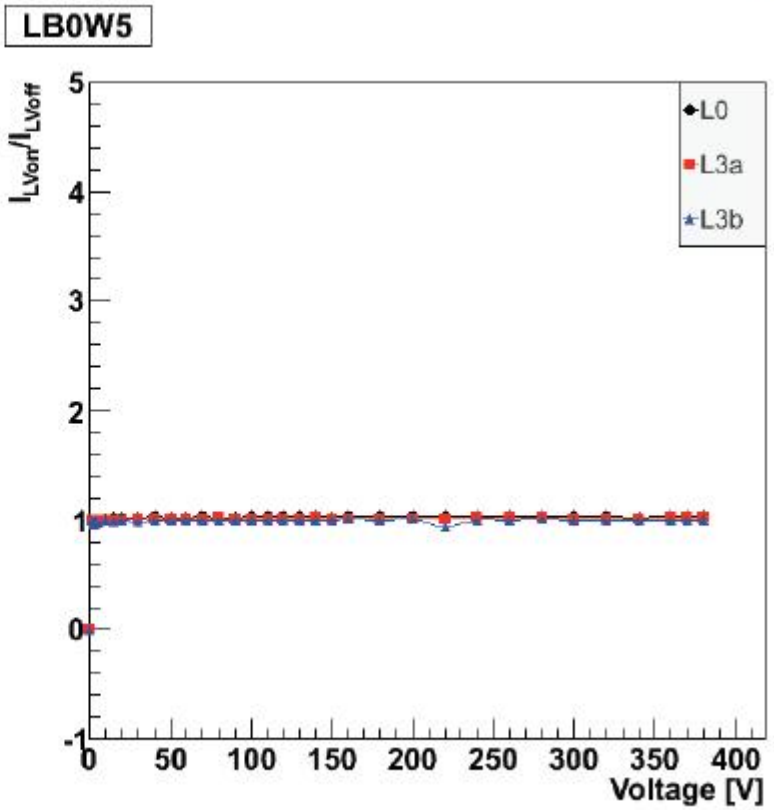

SVT trigger in CDFII: how use silicon information to trigger secondary vertex events

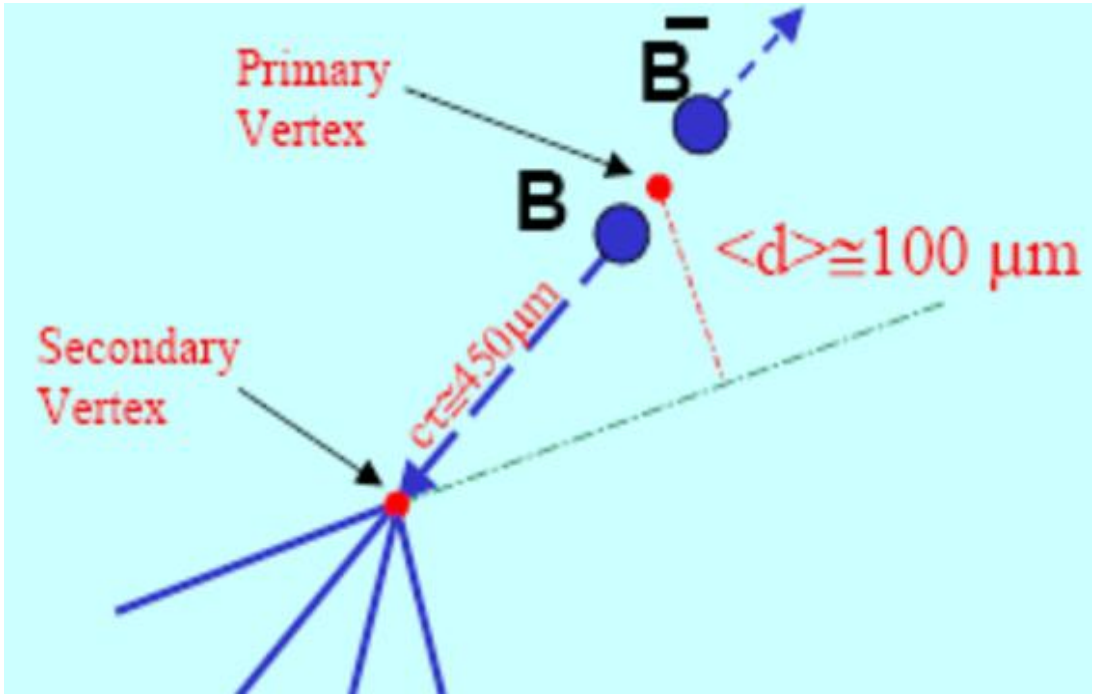

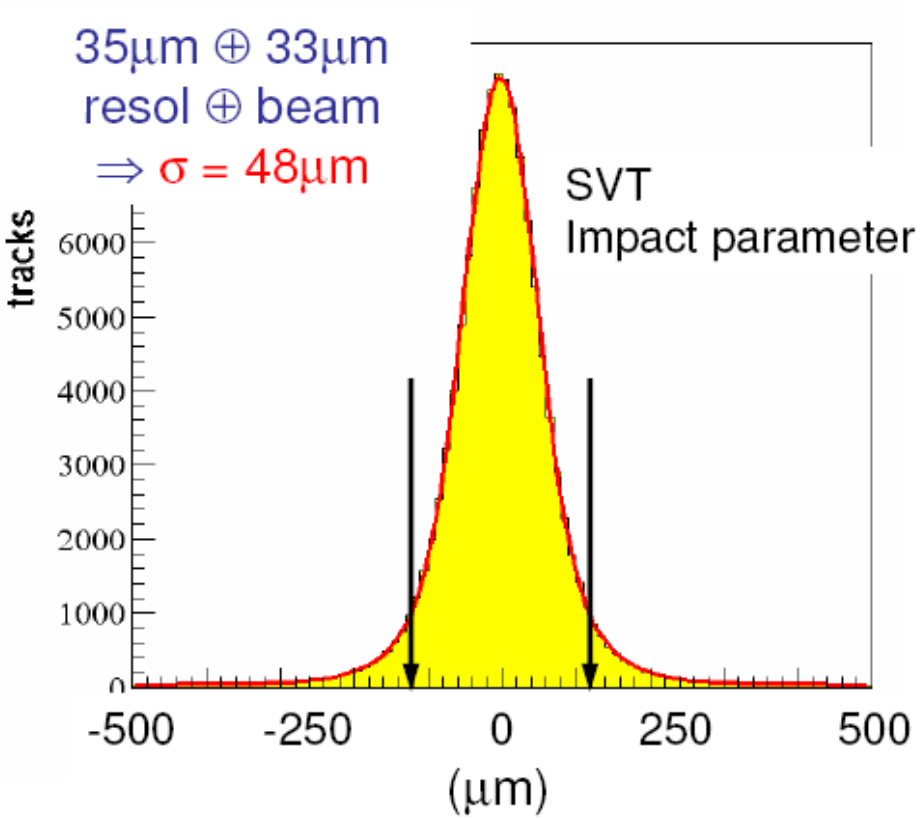

A trigger on secondary vertex: required if we want to look for events with no leptons in the final state, but only tracks.

SVT idea: trigger on events with high impact parameter tracks.

The SVT trigger in CDFII

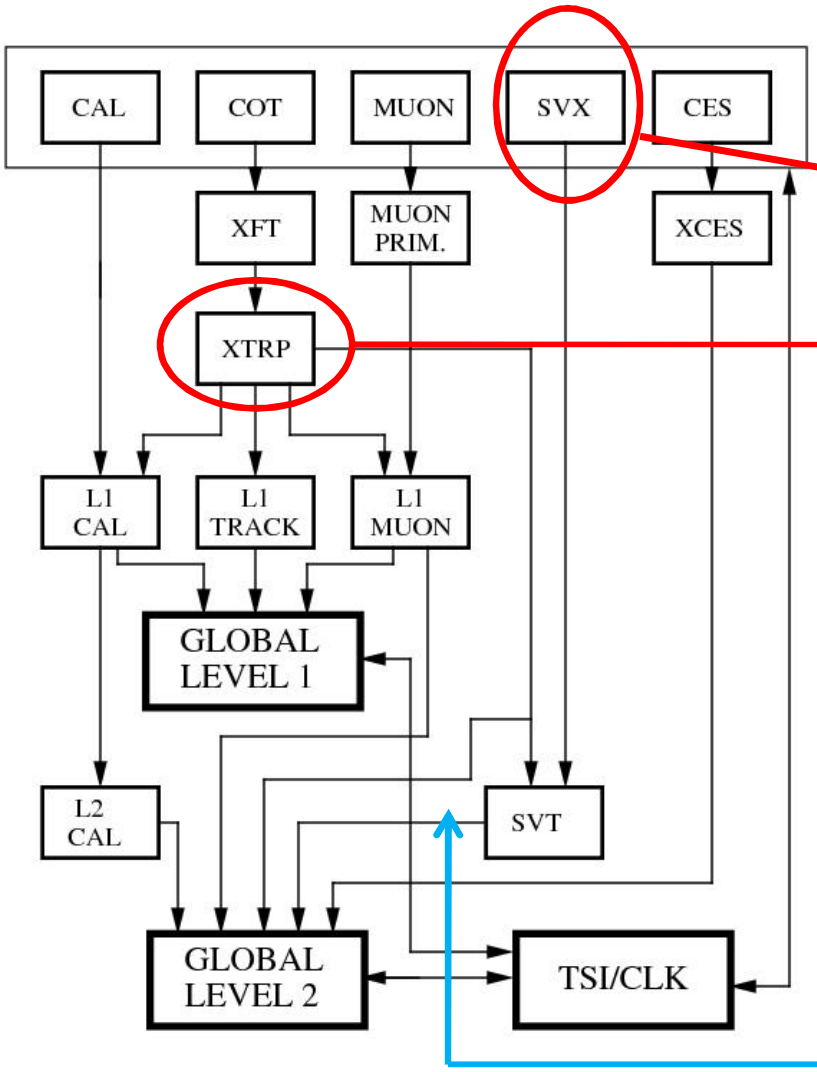

Silicon input: r-phi hits from SVXII

Drift chamber tracks parameters

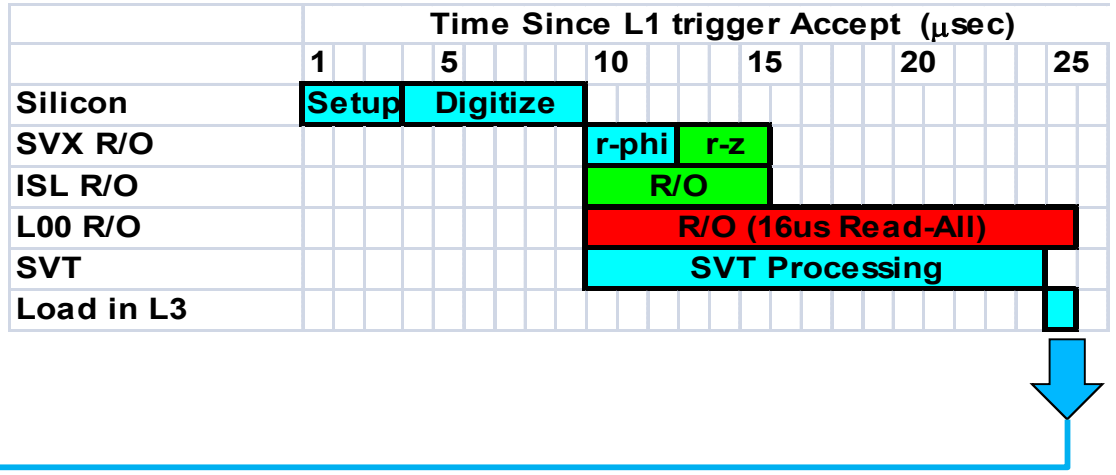

Boards implementation

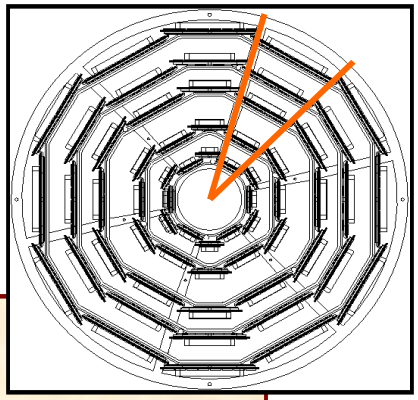

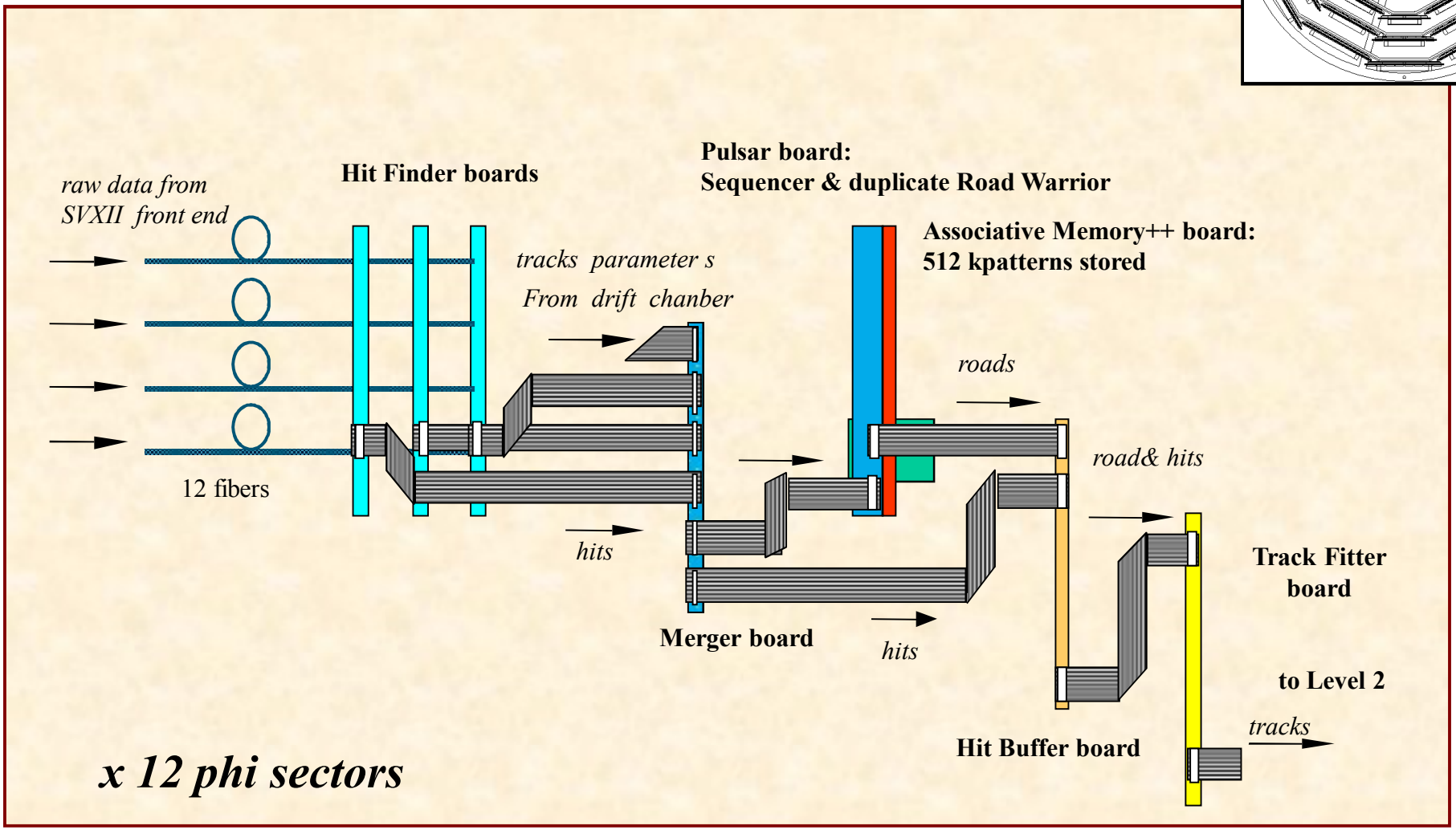

Associative memory: parallel patter recognition

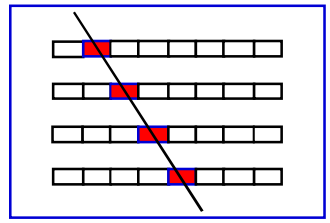

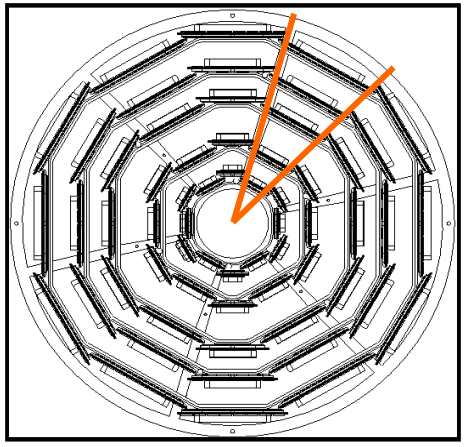

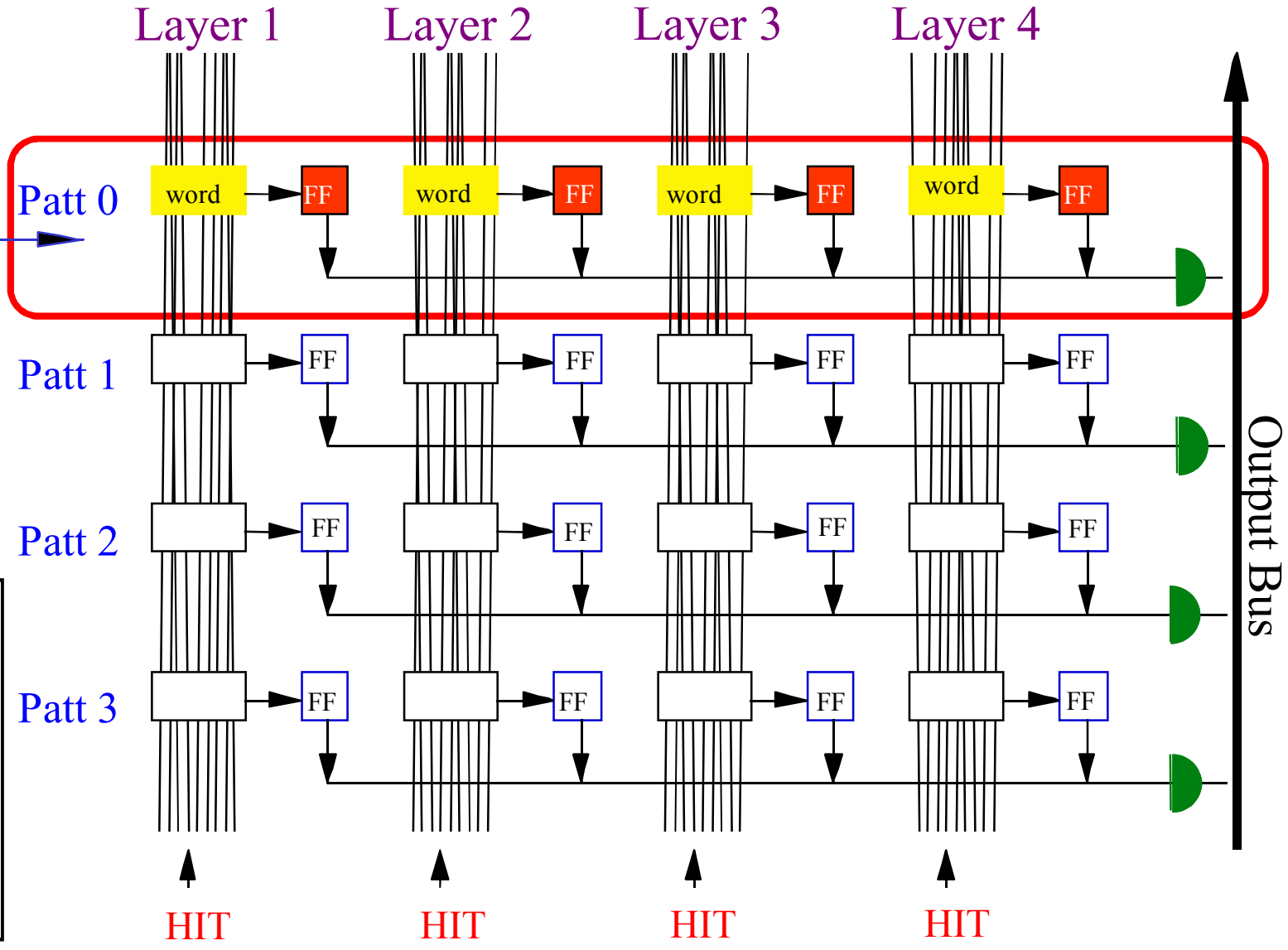

The matching algorithm require at least 4 match over 5

Some results

Bs/Bsbar oscillation measurement:
Phys.Rev. Lett. **97**, 242003 (2006)

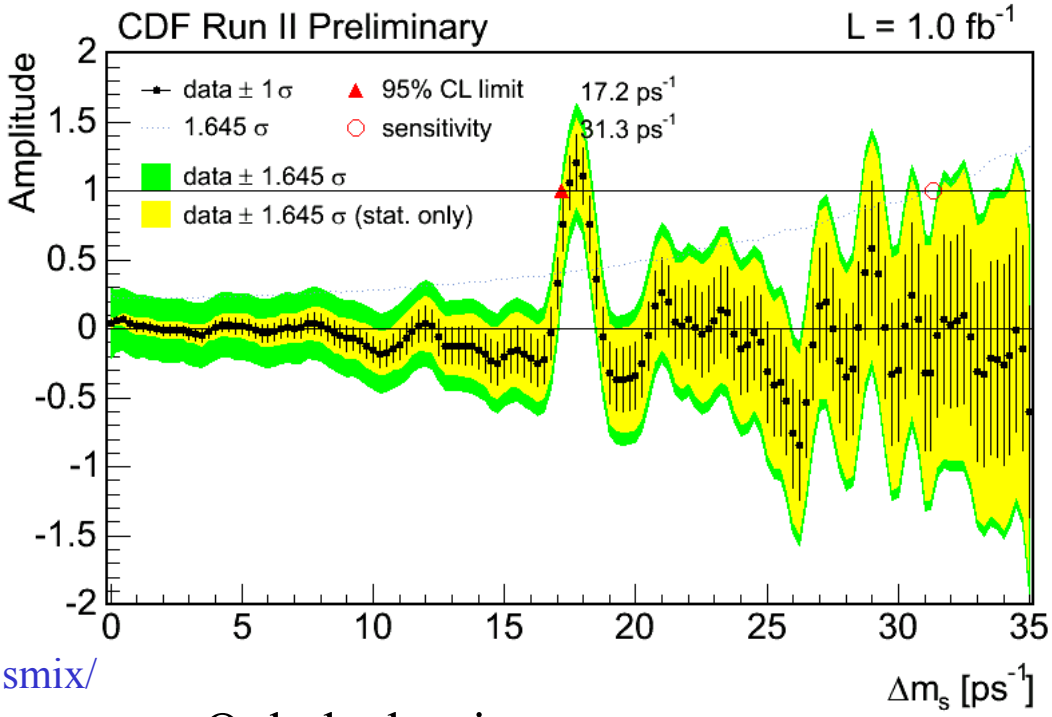

www-cdf.fnal.gov/physics/new/bottom/060831.blessed-Bsmix/

Semi leptonic component

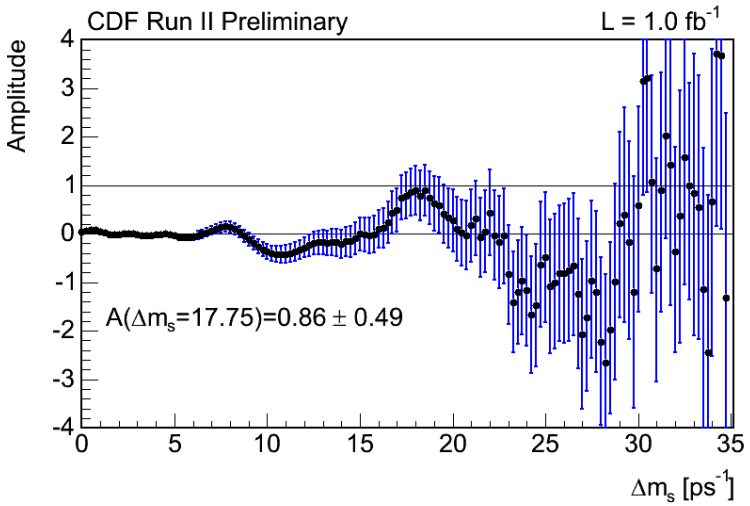

Only hadronic component

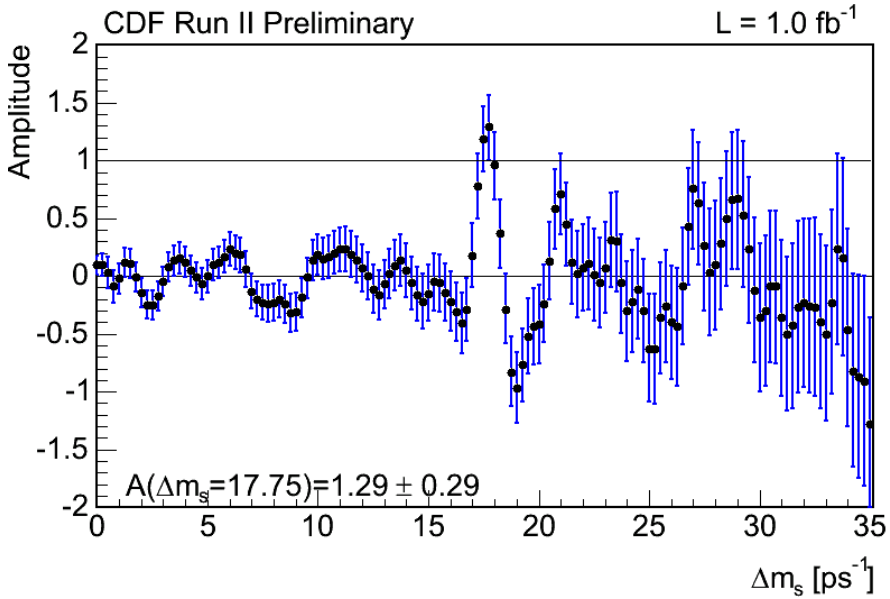

Some results

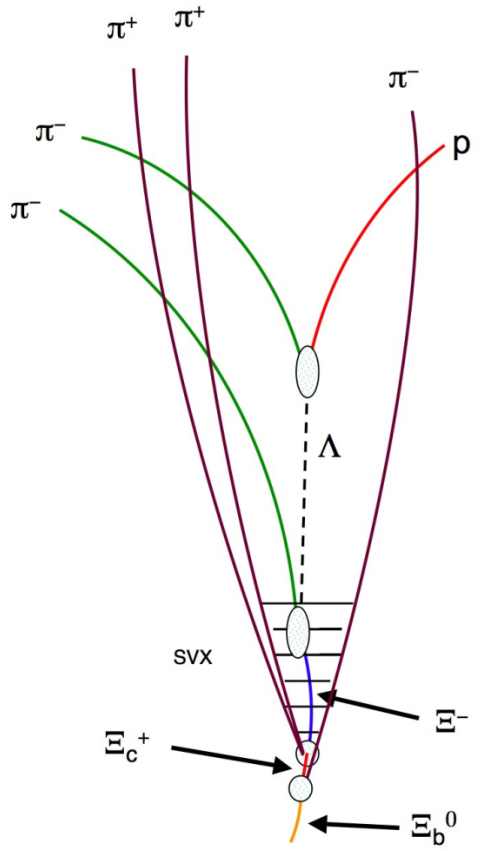

B cascade observation:
Phys. Rev. D **80,** 072003 (2009)

http://www-cdf.fnal.gov/physics/new/bottom/110714.blessed-Xib0/

Conclusions

The CDF Run II silicon detectors were still in quite good shape after 10 years of operation.

The inner layers were showing consistent post-inversion behavior.

The SVXII r-phi readout was successfully used in a hardware secondary vertex trigger (SVT) and allowed to collect huge sample of all hadronic Bs decays.

Back-up slides

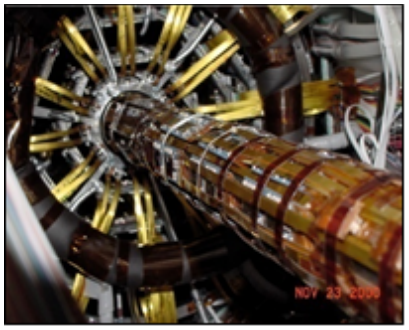
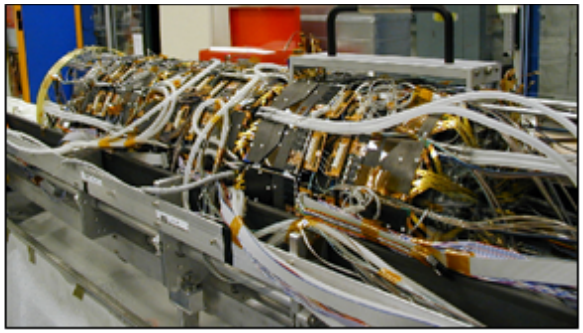
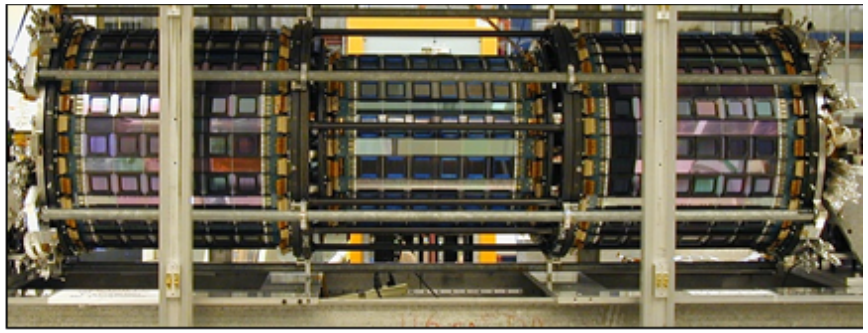

Fermilab accelerators chain

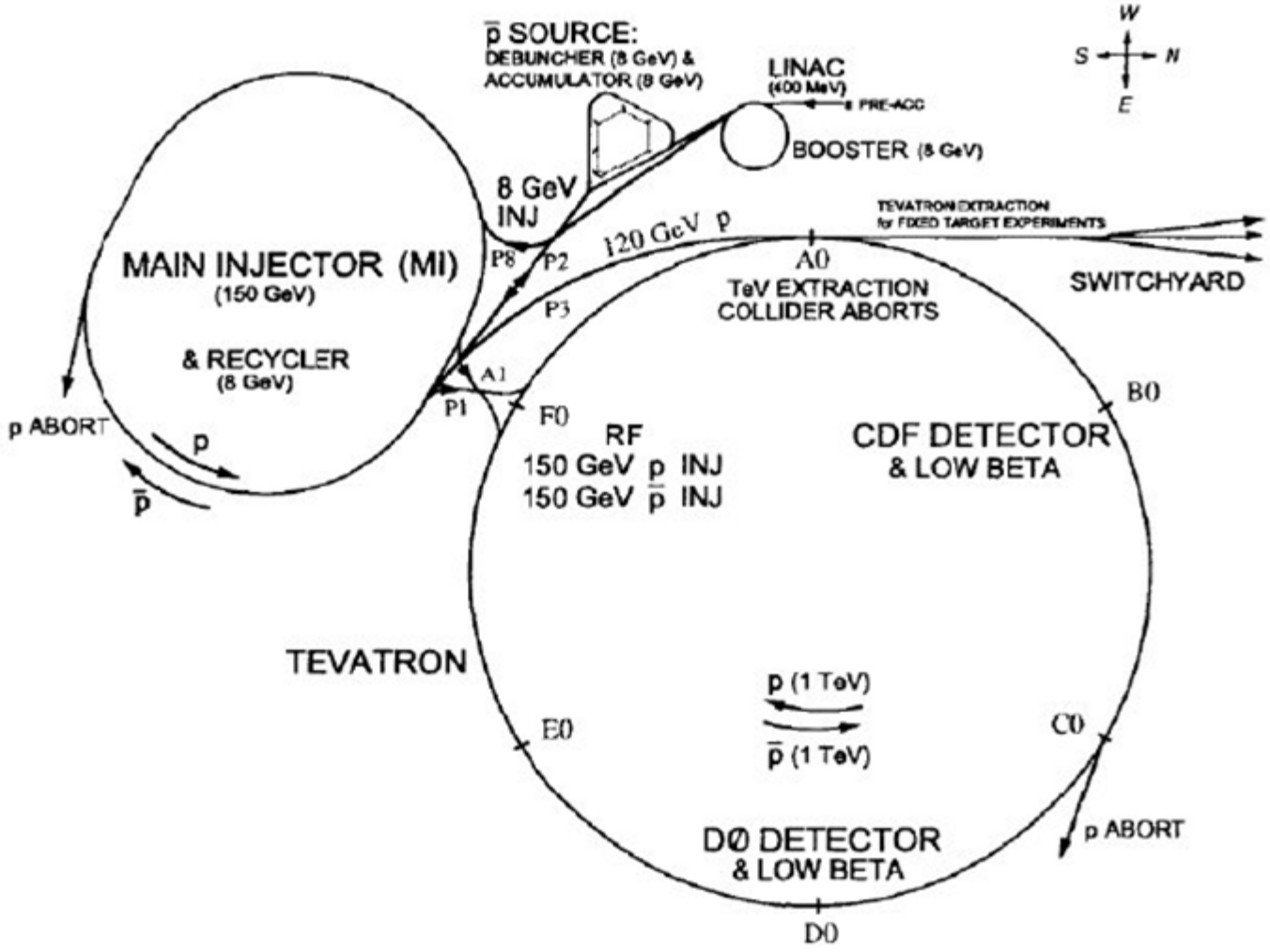

View of the accelerators chain

The Tevatron

Bunches structure

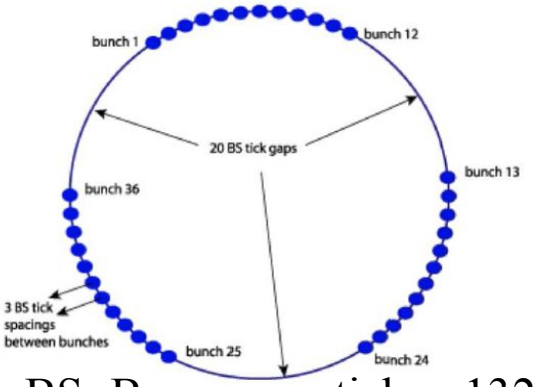

BS=Beam sync ticks =132ns

Initial luminosity record: 4.05 x10^{+32} (cm^{-2} s^{-1})

Mean Pbar production efficiency: ~ 22 x10^{-6}

Mean Pbar Accumulation rate: ~ 25x10^{+10} (hr^{-1})

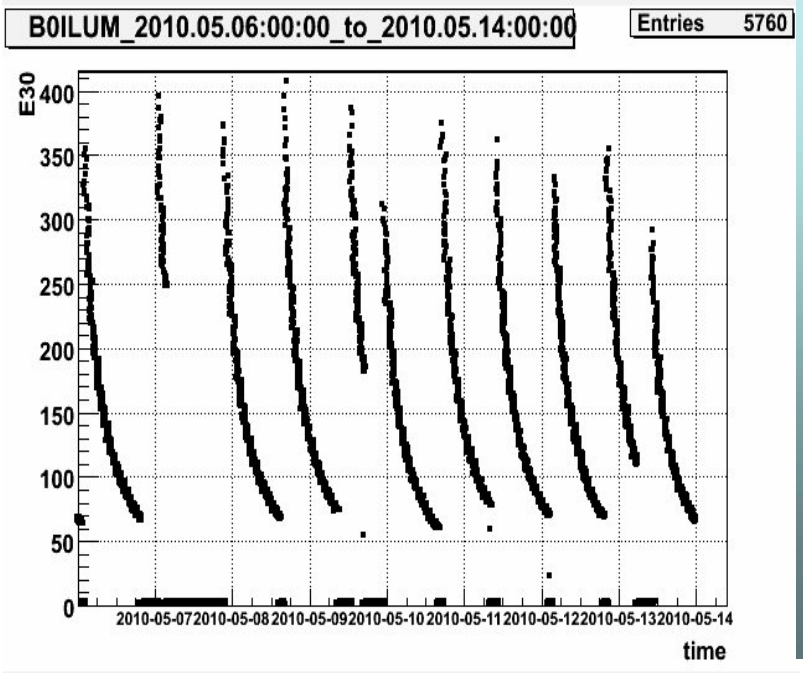

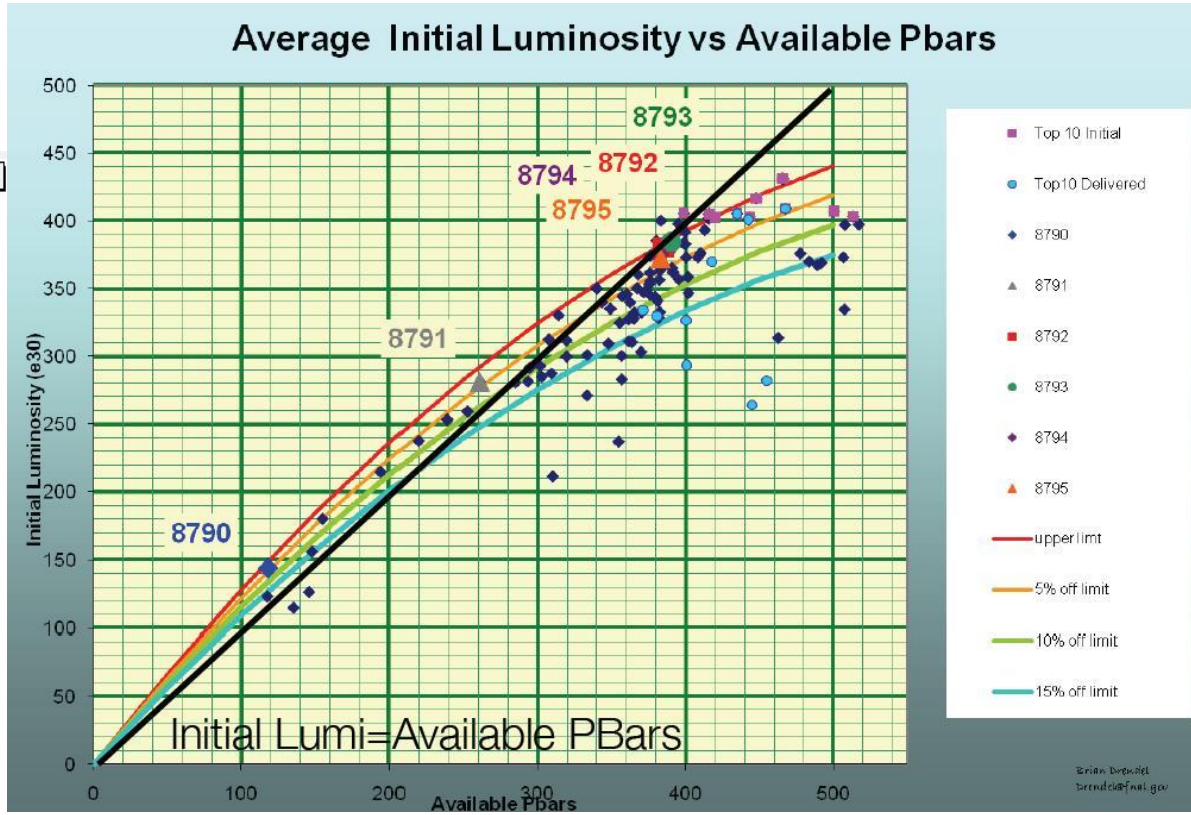

Other Operational Challenges

- **CAEN SY527 Power Supplies**
  - -Communication loss, corrupted read-back, spontaneous switch off,leaking capacitors
  - -A significant fraction of the supplies has been repaired

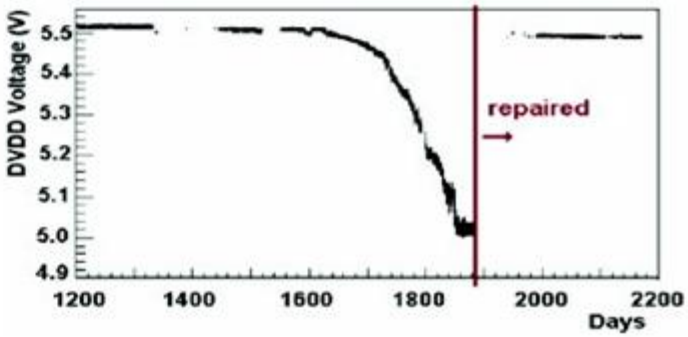

- **ISL Cooling Repairs**
  - -Glycol-water mix turned acidic causing corrosion.
  - -Repairs are challenging, access is possible only from inside the cooling conduits.
  - -Repairs during the 2007 and 2009 shutdowns have significantly improved the tightness of the system

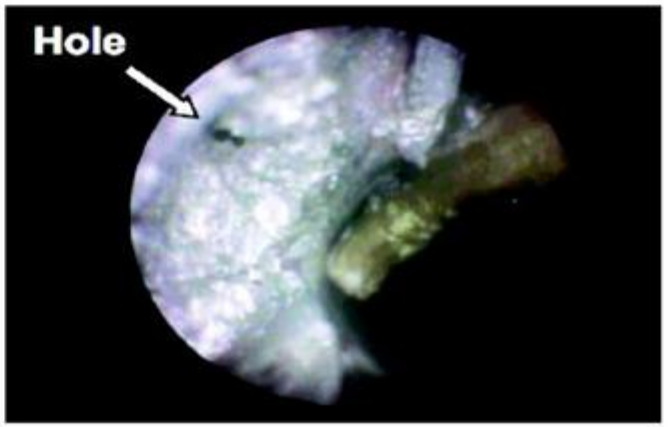

- **Spare electronic components… etc.,etc.**

Measured Radiation Field

- Radiation field measured with TLDs outside the silicon volume in 2002-2003.
- NIM A514 188 (2003)
- Bias current evolution 2002-2004 consistent with this radiation dose

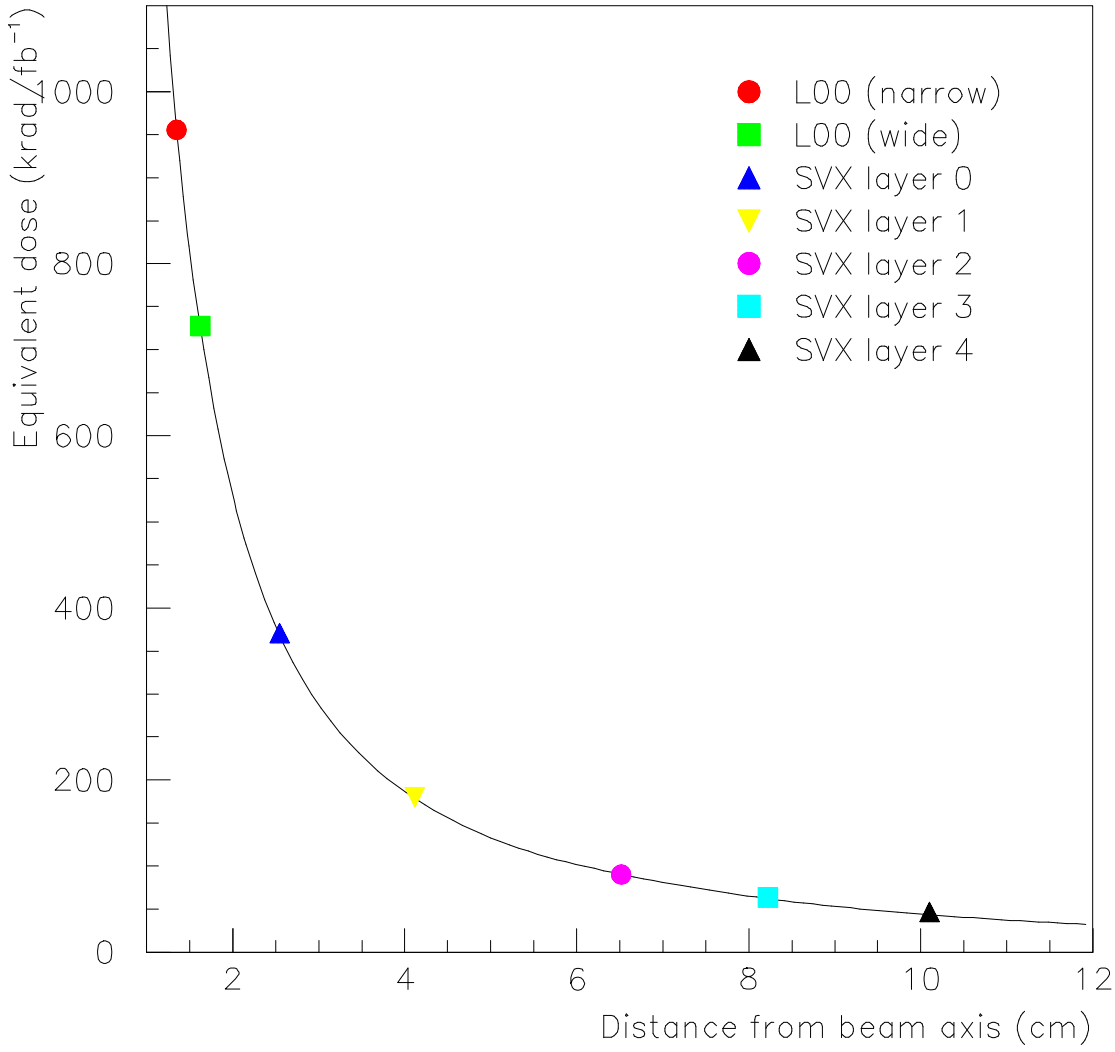

Inversion point

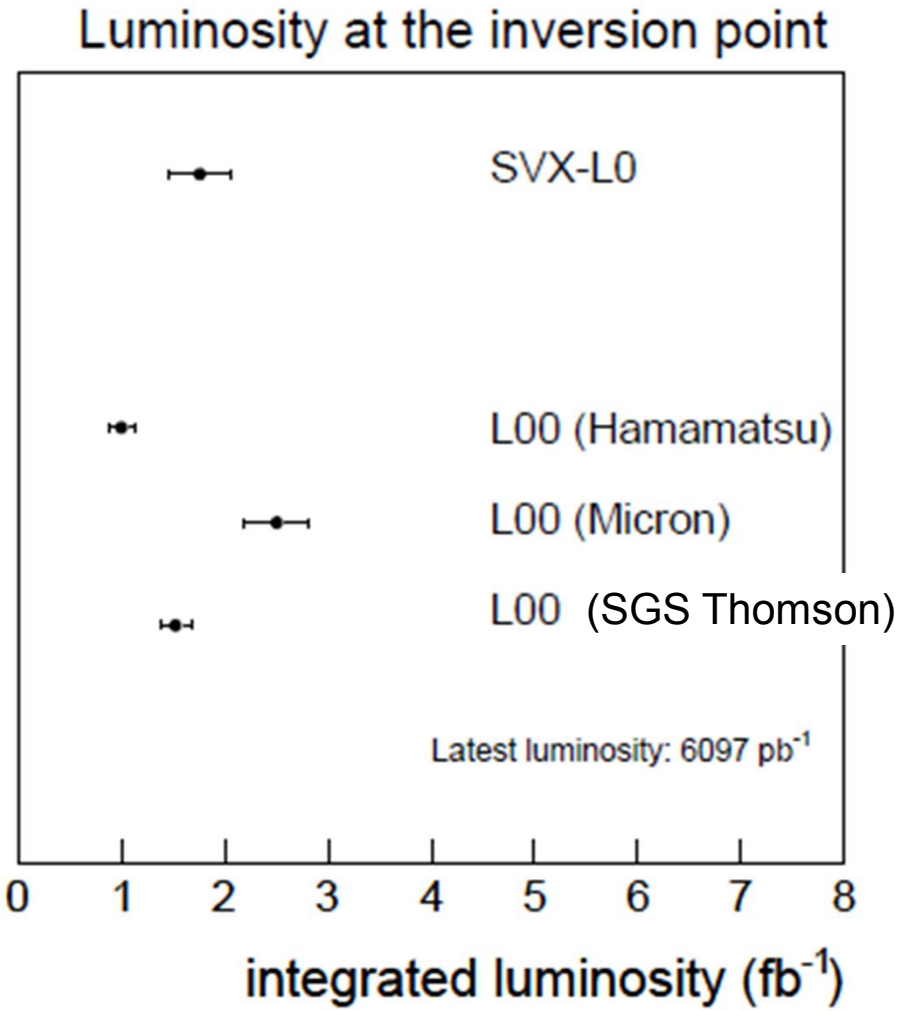

Silicon D.A.Q. for SVX II

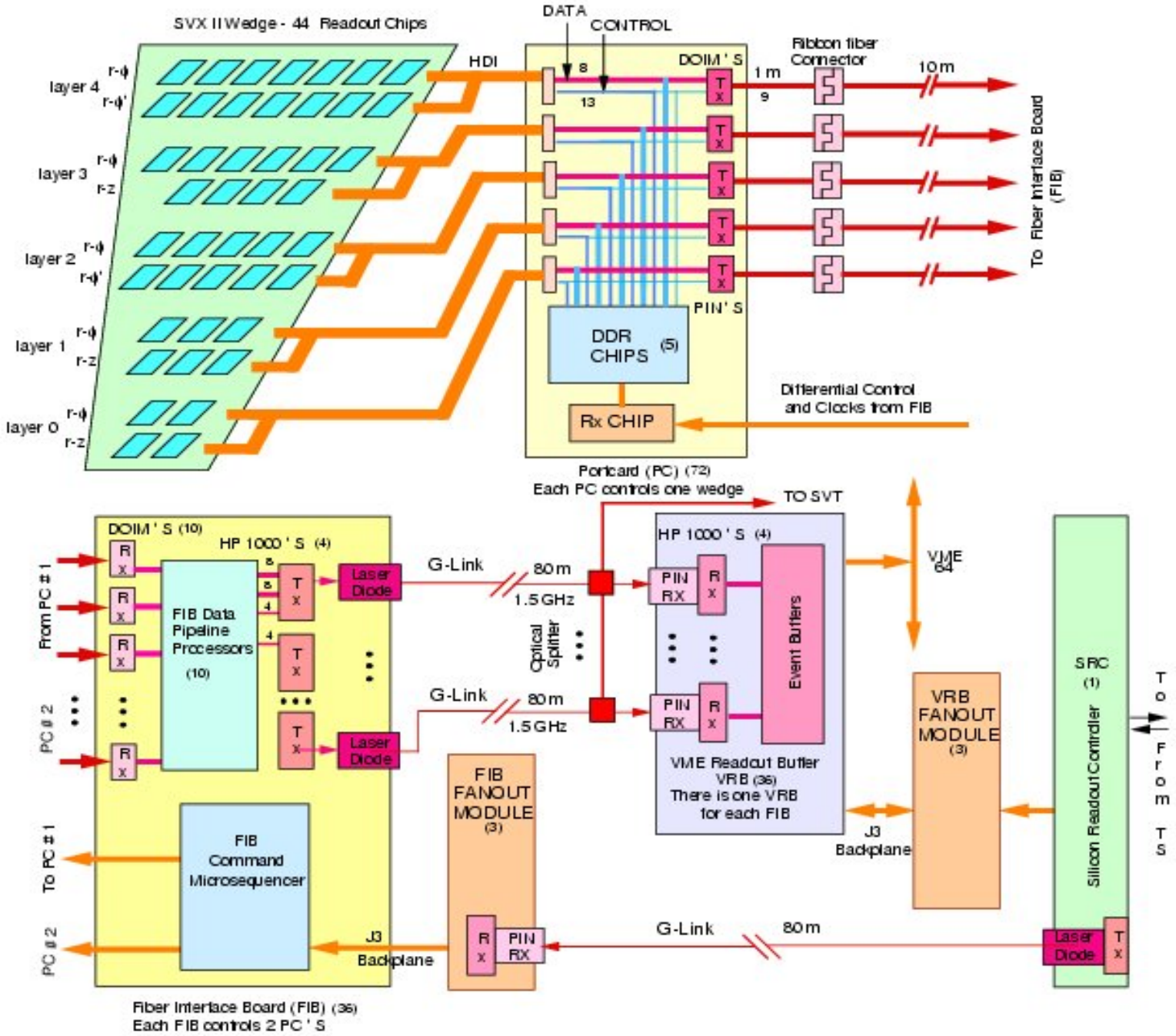

Evolution of Bias currents

- **Fluence in the CDF detector volume is dominated by the physics collisions - related to the delivered luminosity. . Measured using TLDs** (R. J. Tesarek et al. NSS 2003)

- **The fluence – integrated luminosity relationship depends on distance of the sensor to the beam, and is computed by extracting the fluence from the change in bias current.**

- **Using a 95 pb^{-1} data sample collected in 2004, a damage factor of 1.65 ± 0.12 was extracted from bias current data (P. Dong et al. CDF/7275).**

- **Bias evolution and TLD measurements agree well**

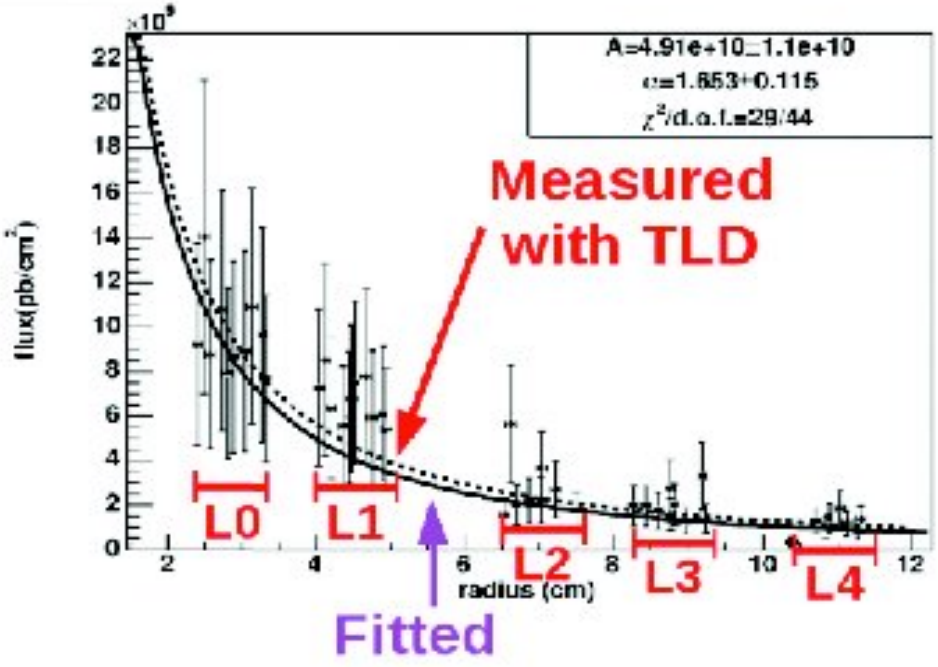

ISL cooling lines

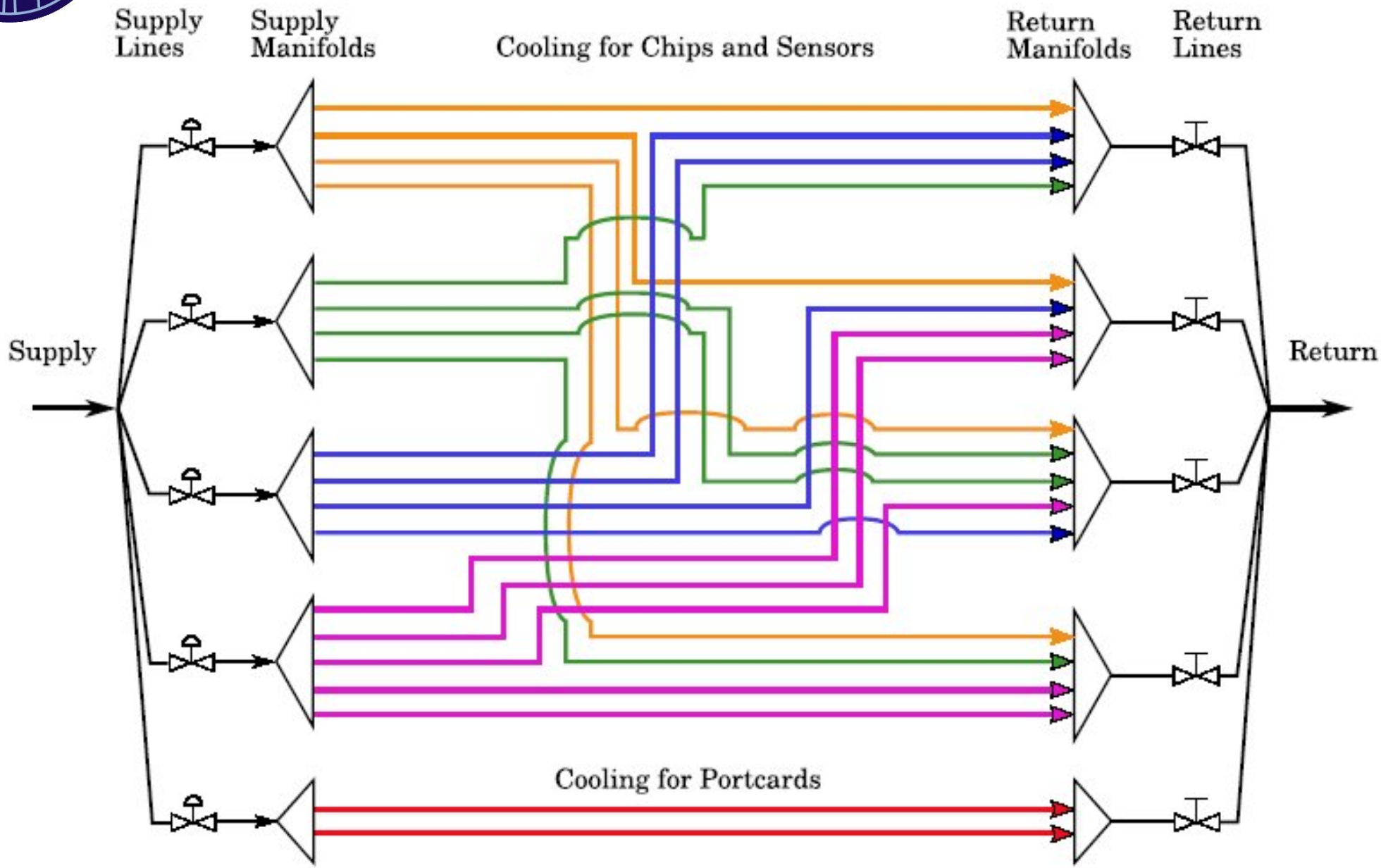

	SVX II	ISL
Detectors	720	900
Half ladders	360	300
Chips	3168	2100
Channels	405,504	268,800
Hybrids	720	300
Port Cards	72	30

SVXII.

Property	Layer 0	Layer 1	Layer 2	Layer 3	Layer 4
number of ϕ strips	256	384	640	768	896
number of Z strips	256	576	640	512	896
number of ϕ chips	2	3	5	6	7
number of Z chips	2	3	5	4	7
stereo angle	90^o	90^o	$+1.2^o$	90^o	-1.2^o
ϕ strip pitch (μm)	60	62	60	60	65
Z strip pitch (μm)	141	125.5	60	141	65
total width (mm)	17.140	25.594	40.300	47.860	60.170
total length (mm)	74.3	74.3	74.3	74.3	74.3
active width (mm)	15.300	23.746	38.340	46.020	58.175
active length (mm)	72.43	72.43	72.38	72.43	72.38
number of detectors	144	144	144	144	144

Table 5.3: Silicon detector mechanical dimensions

Table 1: Summary of L00, SVXII and ISL basic parameters.

Name	Radius (cm)	Orientation	manufacturer
L00 (narrow)	1.35	$r\phi$	SGS Thomson, Micron
L00 (wide)	1.62	$r\phi$	Hamamatsu
SVX L0	2.54	$r\phi$,z	Hamamatsu
SVX L1	4.12	$r\phi$,z	Hamamatsu
SVX L2	6.52	$r\phi$,1.2^o	Micron
SVX L3	8.22	$r\phi$,z	Hamamatsu
SVX L4	10.10	$r\phi$,1.2^o	Micron
ISL L6 Central	22.00	$r\phi$,1.2^o	Hamamatsu
ISL L6 Fwd/Bwd	20.00	$r\phi$,1.2^o	Hamamatsu
ISL L7 Fwd/Bwd	28.00	$r\phi$,1.2^o	Micron

Detector Parameter	SVX′	SVX II
Readout coordinates	r-ϕ	r-ϕ; r-z
Number of barrels	2	3
Number of layers per barrel	4	5
Number of wedges per barrel	12	12
Ladder length	25.5 cm	29.0 cm
Combined barrel length	51.0 cm	87.0 cm
Layer geometry	3° tilt	staggered radii
Radius innermost layer	3.0 cm	2.44 cm
Radius outermost layer	7.8 cm	10.6 cm
r-ϕ readout pitch	60;60;60;55 μm	60;62;60;60;65 μm
r-z readout pitch	absent	141;125.5;60;141;65 μm
Length of readout channel (r-ϕ)	25.5 cm	14.5 cm
r-ϕ readout chips per ladder	2;3;4;6	4;6;10;12;14
r-z readout chips per ladder	absent	4;6;10;8;14
r-ϕ readout channels	46,080	211,968
r-z readout channels	absent	193,536
Total number of channels	46,080	405,504
Total number of readout chips	360	3168
Total number of detectors	288	720
Total number of ladders	96	180

Table 5.1: Comparison of SVX′ and 5-layer SVX II.

ISL

	Atlas	Atlas	L3	L3	Delphi	Delphi	ISL	ISL
side	n	n	p	n	n	n	p	n
S/N	11	17	15	15	12	21	>12	12
RP (μm)	112	112	50	150	100	50	110	146
SP (μm)	56	56	25	50	100	50	55	73
SP/$\sqrt{12}$	16.0	16	7.2	14.4	28.0	14.4	16.0	21.0
σ (μm)	15.6	12.9	7.0	15.0	23.0	10.0	<16.0	<23.0

Table 6.2: Comparison to other silicon detectors with alternate strip readout.

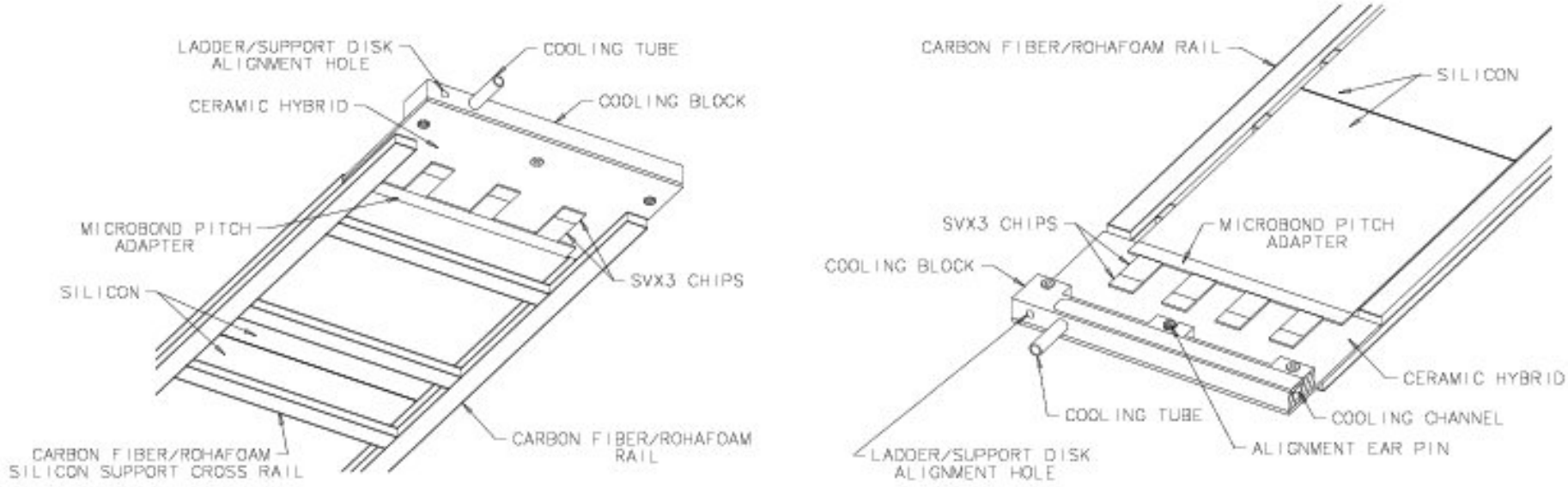

Figure 6.4: A close up view of the readout hybrid on the stereo side of a ladder (left) and the readout hybrid and cooling channel on the axial side of a ladder (right).

END